Published in final edited form as:
J Geophys Res Atmos. 2023 November 27; 128(22): e2023JD038898. doi:10.1029/2023jd038898.

Significant Impact of Reactive Chlorine on Complex Air Pollution Over the Yangtze River Delta Region, China

Xin Yi[1], **Golam Sarwar**[2], **Jinting Bian**[1], **Ling Huang**[1], **Qinyi Li**[3,4], **Sen Jiang**[1], **Hanqing Liu**[1], **Yangjun Wang**[1], **Hui Chen**[1], **Tao Wang**[4], **Jianmin Chen**[5], **Alfonso Saiz-Lopez**[3], **David C. Wong**[2], **Li Li**[1]

[1]Key Laboratory of Organic Compound Pollution Control Engineering (MOE), School of Environmental and Chemical Engineering, Shanghai University, Shanghai, China

[2]Center for Environmental Measurement & Modeling, U.S. Environmental Protection Agency, Research Triangle Park, NC, USA

[3]Department of Atmospheric Chemistry and Climate, Institute of Physical Chemistry Blas Cabrera, CSIC, Madrid, Spain

[4]Department of Civil and Environmental Engineering, The Hong Kong Polytechnic University, Hong Kong, China

[5]Shanghai Key Laboratory of Atmospheric Particle Pollution and Prevention, Department of Environmental Science & Engineering, Fudan University, Shanghai, China

Abstract

The chlorine radical (Cl) plays a crucial role in the formation of secondary air pollutants by determining the total atmospheric oxidative capacity (AOC). However, there are still large discrepancies among studies on chlorine chemistry, mainly due to uncertainties from three aspects: (a) Anthropogenic emissions of reactive chlorine species from disinfectant usage are

Correspondence to: L. Li, Lily@shu.edu.cn.

Author Contributions:
Conceptualization: Xin Yi, Ling Huang, Li Li
Data curation: Xin Yi
Formal analysis: Xin Yi
Funding acquisition: Li Li
Investigation: Xin Yi, Golam Sarwar, Jinting Bian, Ling Huang, Yangjun Wang, Hui Chen, Tao Wang, Li Li
Methodology: Xin Yi, Golam Sarwar, Jinting Bian, Ling Huang, Qinyi Li, Sen Jiang, Hanqing Liu, Yangjun Wang, Hui Chen, Alfonso Saiz-Lopez, David C. Wong, Li Li
Project Administration: Li Li **Resources:** Xin Yi
Software: Xin Yi, Golam Sarwar
Supervision: Golam Sarwar, Ling Huang, Qinyi Li, Yangjun Wang, Hui Chen, Li Li
Validation: Xin Yi
Visualization: Xin Yi, Ling Huang
Writing – original draft: Xin Yi
Writing – review & editing: Xin Yi, Golam Sarwar, Qinyi Li, Tao Wang, Jianmin Chen, Alfonso Saiz-Lopez, David C. Wong, Li Li

Conflict of Interest
The authors declare no conflicts of interest relevant to this study.

Supporting Information:
Supporting Information may be found in the online version of this article.

typically overlooked. (b) The heterogeneous reaction uptake coefficients used in air quality models resulted in certain differences. (c) The co-effect of anthropogenic and natural emissions is rarely investigated. In this study, the Weather Research and Forecasting (WRF)-Community Multiscale Air Quality (CMAQ) modeling system (updated with 21 new reactions and a comprehensive emissions inventory) was used to simulate the combined impact of chlorine emissions on the air quality of a coastal city cluster in the Yangtze River Delta (YRD) region. The results indicate that the new emissions of reactive chlorine and the updated gas-phase and heterogeneous chlorine chemistry can significantly enhance the AOC by 21.3%, 8.7%, 43.3%, and 58.7% in spring, summer, autumn, and winter, respectively. This is more evident in inland areas with high Cl concentrations. Our updates to the chlorine chemistry also increases the monthly mean maximum daily 8-hr average (MDA 8) O_3 mixing ratio by 4.1–7.0 ppbv in different seasons. Additionally, chlorine chemistry promotes the formation of fine particulate matter ($PM_{2.5}$), with maximum monthly average enhancements of 4.7–13.3 μg/m^3 in different seasons. This study underlines the significance of adding full chlorine emissions and updating chlorine chemistry in air quality models, and demonstrates that chlorine chemistry may significantly impact air quality over coastal regions.

Plain Language Summary

The chlorine radical (Cl) plays an important role in the formation of air pollutants such as fine particulate matter and ozone. To better understand its influence, we made significant updates to chlorine chemistry in the widely used chemical transport model Weather Research and Forecasting-Community Multiscale Air Quality (WRF-CMAQ). These updates included the addition of 21 new reactions: 13 gas phase and eight heterogeneous reactions. Additionally, we introduced new emissions sources of Cl_2 and HOCl resulting from the use of chlorine disinfectants. The impact of reactive chlorine emissions from both anthropogenic sources and sea salt on air quality over a coastal city cluster in the Yangtze River Delta was investigated. These results suggest that chlorine affects the atmospheric oxidation capacity, consequently affecting the formation of ozone and fine particulate matter, especially during autumn and winter. Its impact in inland areas is more significant than that in coastal areas owing to intense anthropogenic emissions.

1. Introduction

Chlorine radical (Cl) is a critical atmospheric oxidant that can have significant impact on air quality over coastal regions. Chlorine radicals compete with hydroxyl radicals (OH) to oxidize specific volatile organic compounds (VOCs), although their concentrations are typically two to three orders of magnitude lower than those of OH radicals (Qiu et al., 2019a; Ma et al., 2022). Chlorine radicals can react with VOCs (primarily alkanes, aromatic hydrocarbons, alcohols, and ethers) 1–2 orders of magnitude faster than hydroxyl radicals (Aschmann & Atkinson, 1995; Quack and Willeke, 2010; Wang et al., 2005). Therefore, these substances can enhance (Hong et al., 2020; Qiu et al., 2019a; Simon et al., 2009; Tanaka et al., 2003) or reduce ozone (O_3) and fine particulate matter ($PM_{2.5}$) (J. Y. Li et al., 2021; Zhang et al., 2020) in the troposphere. Cl is primarily produced by photochemical reactions involving HOCl, ClNO, $ClNO_2$, $ClNO_3$, and Cl_2 (R1–R5), the reaction of HCl

with OH (R6), and the NO_3 heterogeneous reaction with particulate chloride (pCl^-) (R7). Currently, we lack the necessary constraints to incorporate the sources of Cl from organic chlorine species. However, they may be expected to be minor contributors compared with inorganic chlorine species.

$$HOCl(g) + h\nu \rightarrow Cl(g) + OH(g) \quad \text{(R1)}$$

$$ClNO(g) + h\nu \rightarrow Cl(g) + NO(g) \quad \text{(R2)}$$

$$ClNO_2(g) + h\nu \rightarrow Cl(g) + NO_2(g) \quad \text{(R3)}$$

$$Cl_2(g) + h\nu \rightarrow 2Cl(g) \quad \text{(R4)}$$

$$ClNO_3 + h\nu \rightarrow Cl(g) + NO_3(g) \quad \text{(R5)}$$

$$HCl(g) + OH(g) \rightarrow Cl(g) + H_2O \quad \text{(R6)}$$

$$NO_3(g) + pCl^- \rightarrow Cl(g) + NO^- \quad \text{(R7)}$$

Some heterogeneous chemical reactions increase the formation of chlorine precursors, indirectly leading to Cl enhancement. For instance, $ClNO_2$ is primarily formed through the heterogeneous reaction of N_2O_5 with pCl^- (Bertram & Thornton, 2009; Roberts et al., 2009). ClNO can be produced only by the interaction of NO_2 with pCl^- (Abbatt & Waschewsky, 1998). Cl_2 can be produced through a wide variety of chemical reactions (Abbatt & Waschewsky, 1998; Deiber et al., 2004; Pratte and Rossi, 2006; Roberts et al., 2008; Rudich et al., 1996). The primary pathways leading to the chlorine precursors are as follows:

$$N_2O_5(g) + H_2O(aq) + pCl^-(aq) \rightarrow ClNO_2(g) + NO_3^- \quad \text{(R8)}$$

$$2NO_2(g) + pCl^- \rightarrow ClNO(g) + NO_3^- \quad \text{(R9)}$$

$$HOCl(g) + pCl^- + H^+ \rightarrow Cl_2(g) + H_2O \quad \text{(R10)}$$

$$ClONO_2(g) + pCl^- \rightarrow Cl_2(g) + NO^- \quad \text{(R11)}$$

$$2OH \cdot (g) + 2pCl^- \rightarrow Cl_2(g) + 2OH^- \quad \text{(R12)}$$

$$O_3(g) + 2pCl^- + H_2O(aq) - Cl_2(g) + 2OH^- + O_2(g)\,. \quad \text{(R13)}$$

$$ClNO_2(g) + pCl^- + H + \rightarrow Cl_2(g) + HONO(g)(pH < 2.0) \quad \text{(R14)}$$

$$ClNO_2(g) + H_2O(aq) \rightarrow pCl^- + NO_3{}^-(g) + 2H^+(pH \geq 2.0) \quad \text{(R15)}$$

Previous studies have suggested that the photolysis of $ClNO_2$ (Sarwar et al., 2014; Haskins, Lee, et al., 2019; Xia et al., 2020), ClNO (Hong et al., 2020) and Cl_2 (Qiu et al., 2019a; Liu et al., 2017) could be the main sources of Cl in coastal megacities, both in the early morning and throughout the day in coastal-megacities (Haskins, Lopez-Hilfiker, et al., 2019). A substantial amount of observational data on $ClNO_2$ has indicated its potentially significant role as a major source of Cl. As chlorine chemistry has been gradually refined in models, diverse results have been obtained in model-based investigations. Qiu et al. (2019a) included heterogeneous chemistry in a Community Multiscale Air Quality model (CMAQ) and found that the photolysis of Cl_2 was the primary contributor of Cl throughout the day, followed by $ClNO_2$ and ClNO. Using a photochemical box model, Liu et al. (2017) derived results similar to those of Qiu et al. (2019a). However, a recent study by Hong et al. (2020) revealed that the majority of Cl is generated from the photolysis of ClNO, with only a minor amount originating from $ClNO_2$, Cl_2, and other reactions. The discrepancies between the results of different studies originate primarily from the parameterization of

Cl sources in heterogeneous chemistry. For instance, Roberts et al. (2008) determined the uptake coefficient of $ClNO_2$ reacting with pCl^- to be 6.0×10^{-3} at pH<2 through laboratory experiments. Haskins, Lee, et al. (2019) obtained a range of γ_{ClNO2} values for acidic particles from 6×10^{-6} to 7×10^{-5} using aircraft-based observations in winter and box models. Recent observational studies have shown that the production of Cl_2 from $ClNO_2$ uptake may be much slower in the ambient troposphere than that initially estimated in the laboratory (Haskins, Lee, et al., 2019), highlighting the large uncertainties in the values derived from laboratory studies when applied in the ambient atmosphere.

Historically, the lack of observational constraints has limited the construction of comprehensive chlorine emission inventories, and the inclusion of different sources in various models has led to significant variations. Sarwar et al. (2014) integrated pCl^- emissions from biomass burning and sea salt sources into the CMAQ model, focusing on the influence of $ClNO_2$ on air quality in the Northern Hemisphere. The findings revealed elevated $ClNO_2$ concentrations in China, suggesting the potentially significant impact of chlorine chemistry in this region. Q. Li et al. (2016) subsequently incorporated a comprehensive inventory of global natural and anthropogenic chlorine emissions (pCl^-, HCl, $ClNO_2$, and inorganic chlorine compounds) developed by Keene et al. (1999) into the WRF-Chem model to investigate the effects of chlorine activation on O_3 in southern China. However, limitations, such as inventory year and resolution, have highlighted the need for an updated chlorine emission inventory in China. Fu et al. (2018) compiled a comprehensive chlorine precursor inventory for 2014 in China, encompassing HCl and pCl^- emissions from coal combustion, industrial processes, biomass burning, and waste incineration. Liu et al. (2018) accounted for HCl and Cl_2 emissions from coal combustion and waste incineration in China. Qiu et al. (2019b) incorporated pCl^- emissions from catering sources into the chlorine emissions inventory for Beijing, revealing that restaurant sources accounted for 75.4% of total pCl^- emissions in urban areas. The generation of pCl^- was mainly due to the volatilization of the added edible salt at high temperatures. Our team compiled a comprehensive emission inventory of reactive chlorine precursors for the Yangtze River Delta (YRD) region (Yi et al., 2021) and China (Yin et al., 2022) in 2018. Our emission inventory included HCl, pCl^-, Cl_2, and HOCl from the source sectors, including coal combustion, industrial processes, biomass burning, waste incineration, cooking, and chlorine-containing disinfectant sources. Overall, the existing chlorine emission inventories and modeling studies in China mainly consider HCl, pCl^-, and Cl_2 emissions from coal combustion, industrial processes, biomass burning, waste incineration, and catering sources. However, emissions from the use of chlorine disinfectants are less frequently included in emission inventories and modeling studies, highlighting a critical gap in the current state of research.

Previous studies have significantly enhanced our understanding of chlorine emissions and their impact on urban air quality. However, there are areas that require further improvement or investigation, specifically the absence of certain anthropogenic and natural sources as well as the lack of agreement concerning the often highly uncertain rates and parameterizations used in chlorine chemistry mechanisms. First, previous model studies may have missed the emissions of chlorine precursors from disinfectants in China. Studies have shown that the use of chlorine-containing disinfectants in swimming pools and cooling

towers can generate significant amounts of Cl_2 and HOCl emissions (Chang et al., 2001; Tanaka et al., 2000; Yi et al., 2021; Yin et al., 2022). Moreover, sea spray emissions from marine sources can potentially affect air quality, especially in coastal city clusters. Dai et al. (2020) used a regional chemical model (WRF-Chem) to investigate the impact of sea salt chlorine particles in the South China Sea on O_3 formation over the Hong Kong-Pearl River Delta and surrounding maritime regions. The findings revealed that, under the influence of marine winds, the photolysis of $ClNO_2$ originating from sea salt chloride, which generates Cl, contributes to an increase in the O_3 mixing ratio in inland regions by 2.0 ppb (4%). This study emphasizes the significant impact of the heterogeneous reactions of reactive nitrogen species on sea salt chloride loss and O_3 formation in coastal areas. However, the combined effects of anthropogenic and marine reactive chlorine emissions remain poorly understood. Finally, the absence of certain gas-phase and heterogeneous reactions in the CMAQ model leads to considerable uncertainties in the results.

Although significant progress has been made in enhancing the understanding of chlorine chemistry through previous studies, substantial uncertainties remain. To improve the accuracy of the impact of chlorine chemistry on air quality, this study focused on three key aspects: (a) We have updated the chlorine chemistry by adding 21 new reactions including 13 gas-phase and eight heterogeneous chlorine reactions; we have determined reliable uptake coefficients of pCl^- and various substances in heterogeneous reactions through sensitivity experiments. (b) Our study addressed the anthropogenic sources of reactive chlorine, including Cl_2 and HOCl, emitted from chlorine-containing disinfectants. Notably, these sources were overlooked in previous studies conducted in China. (c) In addition to examining the impact of anthropogenic emissions, we comprehensively investigated the influence of natural (sea salt) and anthropogenic chlorine emissions on air quality. This broader approach provides a more holistic understanding of the impact of chlorine chemistry on air quality in the YRD region. The incorporation of these complete chlorine emission sources and substances, along with updated chlorine chemistry, significantly enhanced the reliability of our study for evaluating the impact of chlorine chemistry on air quality in the YRD region.

2. Methodology

2.1. Observational Data

The air quality data used in this study were obtained from the National Urban Air Quality Real-Time Release Platform of the China National Environmental Monitoring Center (http://www.cnemc.cn/). This study focused on hourly data obtained from 206 monitoring stations in the YRD region (indicated by the red dots in Figure 1).

The availability of observational data on chlorine-containing compounds in the YRD region is limited. Therefore, we conducted a comprehensive literature review and collected studies that provided observations on Cl species in the YRD region. These observational data were then compared with the model-predicted values for the chlorine-containing compounds. Section 3.1 of the study focuses on discussing the comparisons between the observed and model-predicted chlorine species. This analysis aims to assess the performance of the model in reproducing observed levels of chlorine-containing compounds in the YRD region.

By comparing the model predictions with available observational data, we can evaluate the accuracy and reliability of the model's representation of chlorine chemistry in the atmosphere.

2.2. Modeling System

In this study, the Weather Research and Forecasting (WRF version 3.7) model (Skamarock et al., 2008) provided the meteorological data to drive the CMAQ model (version 5.3.1). The final NCEP/NCAR reanalysis data (1° × 1°) provided initial meteorological fields and WRF boundary conditions. For this research, we utilized three nested domains with horizontal grid resolutions of 36, 12, and 4 km for the WRF and CMAQ models (Figure 1). Domain 1 (D1) covers a wide region, including China, Japan, the Korean Peninsula, parts of India, and Southeast Asia, with a grid spacing of 36 km × 36 km; Domain 2 (D2) covers eastern China with a grid spacing of 12 km × 12 km; and Domain 3 (D3), with a grid spacing of 4 km × 4 km, covers the YRD (Anhui, Zhejiang, Jiangsu, and Shanghai provinces) and some surrounding areas. The chemical boundary conditions for the CMAQ model were obtained from the Model for Ozone and Related Chemical Tracers, version 4 (MOZART-4) (https://www2.acom.ucar.edu/gcm/mozart-4). CB6 and AERO7i were implemented as the gas-phase and aerosol mechanisms in the CMAQ model, respectively (Cho et al., 2021; Yarwood et al., 2010).

Emissions of conventional pollutants from anthropogenic sources were obtained from the Multi-resolution Emission Inventory for China (MEIC, http://www.meicmodel.org/), and the simulation of each month of the emission inventory for the YRD region was developed by our research group and is described in detail by Huang, Wang, et al. (2021). The Model of Emissions of Gases and Aerosols from Nature (MEGAN3.1) was used to calculate emissions from biogenic sources (Guenther et al., 2006). Additionally, a more comprehensive inventory of anthropogenic chlorine emissions in the YRD region was developed, including various chlorine-containing species such as Cl_2, HOCl, HCl, and pCl^-, as well as multiple source categories, including coal combustion, industrial processes, waste incineration, biomass burning, cooking, and the usage of disinfectants (Yi et al., 2021). In the YRD region, the emissions of HCl, pCl^-, Cl_2, and HOCl in 2018 were estimated to be 20,424 t, 15,719 t, 1,556 t, and 9,331 t, respectively. Compared with previous studies, the inventory used in this study is up-to-date and covers 2018. Additionally, previous chlorine chemistry modeling studies in China did not consider the emissions of Cl_2 and HOCl from chlorine disinfectant sources. The Cl_2 and HOCl, emitted from chlorine-containing disinfectants were estimated at 1236.7 t and 9,331 t, contributing 79.5% and 100% to the total emissions of Cl_2 and HOCl, respectively. Notably, these sources were overlooked in previous studies conducted in China. The sea salt module of the CMAQ model was used to simulate sea spray emissions from the ocean (Gantt et al., 2015). These emissions are categorized into the following species: Cl^-, Na^+, SO_4^{2-}, Ca^{2+}, Mg^{2+}, and K^+ (Millero, 2013). Sea-salt contributes around 15,207 t (1032 t in February, 733 t in April, 2059 t in July, and 1245 t in November, respectively) of pCl^- emissions annually based on the CMAQ sea-salt online module, which is equivalent to anthropogenic sources, but does not directly contribute any emissions of Cl_2 and HOCl.

The modeling period for this study covered February, April, July, and November 2018, representing winter, spring, summer, and autumn, respectively. The simulation for each month included a 14-day spin-up period. Two numerical experiments were conducted to investigate the influences of anthropogenic and natural chlorine emissions on air quality. These experiments are referred to as the Base case and CL case. In the Base case, the default chlorine chemistry of CB6 and AERO7i was employed, and no chlorine emissions were considered. Table S1 in Supporting Information S1 provides an overview of the chlorine chemical reactions involved in this mechanism, including 30 gas-phase and two heterogeneous reactions. The key chlorine-containing compounds were Cl_2, HOCl, HCl, pCl^-, $ClNO_3$, $ClNO_2$, ClO, and FMCl. In the CL experiments, updates were made to the gas phase and heterogeneous chemical reactions in the WRF-CMAQ model. The updates are listed in Table S2 in Supporting Information S1.

In addition to the chemistry described in Table S1 in Supporting Information S1, the updated chlorine mechanism includes 13 gas-phase and 8 heterogeneous reactions involving chlorine. The newly added chlorine-containing compound ClNO and its photolysis, as well as the reactions between Cl and aldehydes (GLY and MGLY), acids (AACD and FACD), ketones (ACET), and inorganic substances (NO, HO_2 and NO_3), were included. The newly added heterogeneous reactions involve the interactions of pCl^- with different chemical species, leading to the generation of Cl_2, ClNO, and $ClNO_2$. New heterogeneous reactions of pCl^- with OH, NO_2, NO_3, O_3, $ClNO_3$, HOCl, and $ClNO_2$ were performed, and Cl_2 and ClNO were identified as the main reaction products. The choice of the uptake coefficient significantly affects the concentration of products. The uptake coefficients for pCl^- reacting with OH (Choi et al., 2020; Wang et al., 2019), NO_2 (Abbatt & Waschewsky, 1998; Choi et al., 2020; Qiu et al., 2019b), NO_3 (Rudich et al., 1996; Zelenov et al., 2014), HOCl (Lawler et al., 2011; Pratte and Rossi, 2006), and $ClNO_3$ (Deiber et al., 2004) showed minor differences, leading to the retention of their values without modification. However, notable discrepancies were observed in the uptake coefficients for pCl^- reacting with O_3 and $ClNO_2$. For heterogeneous reactions between pCl^- and O_3, the uptake coefficients ranged from 5×10^{-8} to 10^{-4}, as reported by Abbatt and Waschewsky. (1998). Chen et al. (2022) used uptake coefficients of 10^{-3}, 10^{-4}, and 10^{-5} for pCl^- and O_3 in their box model, leading to significant overestimation of Cl_2 concentrations. We conducted sensitivity experiments using the uptake coefficient chosen by Qiu et al. (2019b) and found that it overestimated Cl_2 compared with the observed data; thus, we did not select it for our study. Therefore, we have chosen $\gamma = 1.3 \times 10^{-6}$ from Il'in et al. (1991), as this value is more suitable for our study.

F. B. Li et al. (2023) used observational methods in Shanghai and Changzhou to indicate that the formation of Cl_2 in Changzhou mainly comes from the reaction of $ClNO_2$ and pCl^- on acidic aerosols. The formation of Cl_2 at night in Shanghai is mainly related to the reaction of $ClNO_2$ and pCl^-, so there is a significant relationship between the reaction of $ClNO_2$ and pCl^-. Roberts et al. (2008) conducted laboratory experiments and reported an uptake coefficient of $\gamma = 2.65 \times 10^{-6}$ at pH ≥ 2 s and $\gamma = 6.0 \times 10^{-3}$ at pH < 2. Haskins, Lee, et al. (2019) used aircraft measurements during winter over the eastern United States and analyzed the data using a chemical box model with heterogeneous reactions of $ClNO_2$ and pCl^-; and reported 2–3 orders of magnitude lower than those reported by Roberts et al. (2008), even at pH < 2. Both studies show minor differences at pH ≥ 2, but γ_{ClNO2}

differs substantially at pH < 2. However, strongly acidic conditions are less prevalent in the atmospheric environments in China. While aerosol pH levels in the U.S. are highly acidic (pH = 0–2), aerosol pH levels in China tend to be less acidic (pH = 2.5–6) (Zhou, et al., 2022). We have conducted additional sensitivity experiments (see the attached Supporting Information S1) to examine the impact of $\gamma_{ClNO2} = 6.0 \times 10^{-6}$ at pH < 2. The results show that the selection of this uptake coefficient had a minor impact on Cl_2 in both summer and winter. Overall, the heterogeneous reaction of $ClNO_2$ with pCl^- had a relatively small impact on Cl_2. The CL case considered chlorine emissions from both anthropogenic and oceanic sources. The impact of chlorine emissions and chemistry on the formation of O_3 and $PM_{2.5}$ was quantified by comparing the results of the Base and CL experiments.

2.3. Calculation of Atmospheric Oxidation Capacity

To assess the effect of chlorine chemistry on overall atmospheric oxidation, we used the concept of atmospheric oxidation capacity (AOC: molecules cm^{-3} s^{-1}), which symbolizes the quantity of carbon oxidized in the atmosphere over time. AOC was calculated using Equation 1 (Q. Y. Li et al., 2020):

$$\mathrm{AOC} = \sum_{i=1}^{m} \left([OX_i] \times \sum_{j=1}^{n} ([C_j] \times K_{i,j}) \right) \quad (1)$$

where m is the number of oxidants (Cl, NO_3, O_3, and OH), n is the number of reactant (CO and VOC) species, $[OX_i]$ is the concentration of oxidant i (molecules cm^{-3}), $[C_j]$ is the concentration of reactant j (molecules cm^{-3}), and $K_{i,j}$ is the reaction rate constant (cm^3 $molecules^{-1}$ s^{-1}). The chemical reactions and the corresponding rate constants are listed in Table S3 in Supporting Information S1.

3. Results and Discussion

3.1. Model Performance Evaluation

Table 1 shows the model performance evaluation results for O_3 and $PM_{2.5}$ in both the Base and CL experiments, using urban monitoring station data averaged across the YRD region. The O_3 simulations in February, April, and July in the Base experiment exhibited underestimation and a slight overestimation in November, which may be mainly related to NO_x or VOCs emissions. The Base experiment also underestimated $PM_{2.5}$, except in July and November, when an overestimation occurred. Despite this, the low bias, high consistency index, and correlation coefficient values for each month suggest acceptable O_3 and $PM_{2.5}$ model performance. The discrepancies between the simulated values and air quality measurements can be attributed to two main factors. First, uncertainties in the emissions inventory, which typically includes conventional air pollutants such as SO_2, NO_x, $PM_{2.5}$, VOCs, NH_3, etc but often lacks data on chlorine species such as HCl, pCl^-, Cl_2, and HOCl. Second, there is an inadequate representation of chlorine chemistry in the model, including the absence of detailed gas-phase chlorine reactions and an insufficient mechanism for secondary organic aerosol formation (Y. Li et al., 2021; Qiu et al., 2019a; Shang et al.,

2021). Despite these challenges, the model performance, when compared to the statistics reported in previous studies and proposed benchmarks, is considered acceptable (Hong et al., 2020; Huang, Zhu, et al., 2021).

Notably, the CL experiment simulation, compared to the Base experiment, led to improved O_3 and $PM_{2.5}$ model performance in February and April, with a reduced overall monthly average deviation in the model simulation. Remarkably, the root mean square error, index of agreement, and *r* values showed minimal differences between the Base and CL experiments, indicating that model performance improved in the CL experiments.

However, the measurements of chlorine-containing substances in the YRD region are limited. Therefore, this study aimed to address this knowledge gap by collecting literature and monitoring data on chlorine-containing substances, as presented in Table 2. Observational data for HCl and pCl^- at the Changzhou Station in 2018 were obtained. The simulated concentrations of HCl and pCl^- at Changzhou station were lower than the observed data because of the underestimation of emissions around the monitoring station. Nevertheless, the CL simulation, when compared to the Base scenario, where HCl and pCl^- concentrations were essentially zero, exhibited some improvement in simulating the performance of HCl and pCl^-. In a study conducted by Xia et al. (2020) at the Xianlin campus of Nanjing University in April, observations were made on the concentrations of $ClNO_2$, Cl_2, and HOCl were observed. Under the CL simulation scenario, the simulated concentrations of these substances closely matched the observed values with relatively minor differences. It is worth noting that the CL simulation may have slightly underestimated the concentrations of $ClNO_2$ and HOCl while overestimating the concentration of Cl_2. In general, the simulated concentrations of chlorine-containing substances in the CL experiment exhibited substantial improvement compared to the Base experiment. This finding strongly suggests that the simulation conducted in the CL experiment provides a better representation of the actual atmospheric environment.

3.2. Impacts of Chlorine Chemistry on Chlorinated Species

3.2.1. HCl—The monthly spatial distribution of HCl concentrations in the CL experiment is shown in Figures 2a–2d. HCl exhibited a comparable spatial pattern during autumn and winter, characterized by elevated concentrations in the southern coastal region of Zhejiang Province. Within marine areas, the formation of HCl is enhanced by a heterogeneous reaction between pCl^- and HNO_3 or H_2SO_4 as described by Saul et al. (2006). During spring and summer, elevated HCl concentrations were prominently observed in Anhui, southern Jiangsu Province, and the coastal regions. This phenomenon can be attributed to the specific factors prevalent in these areas. The Anhui and Jiangsu provinces, which are characterized by relatively advanced agricultural practices, experienced more substantial instances of biomass burning. Consequently, these activities contributed to the heightened emissions of HCl and pCl^-. In coastal regions, the presence of ocean spray aids in the introduction of pCl^- into the atmosphere. Moreover, the warmer temperatures prevalent during spring and summer facilitated the conversion of pCl^- to HCl. Hence, this conversion process, influenced by climatic conditions, leads to increased HCl concentrations in coastal areas. Comparing the CL experiment with the Base case (Figures 3a–3d), the disparity

in HCl concentrations signified a substantial increase in the southeastern coastal area of Zhejiang Province during autumn and winter, primarily attributed to the transformation of chlorine present in sea salt aerosols. Furthermore, the conversion of pCl^- to HCl exhibited a greater tendency toward sea salt during the spring and summer. These findings indicate that the generation of HCl from marine sources surpasses that from anthropogenic sources during spring and summer, with marine air masses transporting a higher concentration of pCl^- to the mainland than during autumn and winter.

3.2.2. pCl^-—Figures 2e–2h present the spatial distribution of monthly average pCl^- concentrations across different months. Certain regions, particularly in northern Anhui and southern Jiangsu province, exhibit higher monthly average pCl^- concentrations, reaching a peak value of 4.2 $\mu g/m^3$. Notably, spring and summer show lower monthly average pCl^- concentrations compared to autumn and winter. This can be attributed to two factors. First, spring and summer coincide with the sowing and growth of crops, resulting in a relatively lower proportion of biomass burning. Second, the higher relative temperatures during spring and summer facilitate the conversion of pCl^- into HCl, whereas such conversion is less prevalent during in autumn and winter. The divergence between the CL and Base experiments for pCl^- (Figures 3e–3h) highlights the substantial influence of anthropogenic emissions on inland pCl^- concentrations, particularly during autumn and winter.

3.2.3. $ClNO_2$—Figures 2i–2l illustrates the spatial distribution of the monthly simulated $ClNO_2$ concentrations. The generation of $ClNO_2$ occurs via a heterogeneous reaction between pCl^- and N_2O_5. During autumn and winter, Anhui and southern Zhejiang provinces exhibited higher average monthly $ClNO_2$ concentrations than other regions. This can be primarily attributed to elevated pCl^- emissions resulting from biomass burning. Conversely, the monthly average $ClNO_2$ concentrations in the YRD region were generally lower in spring and summer. The concentration of $ClNO_2$ in the coastal area in spring and summer was significantly lower than that in other months, owing to unfavorable meteorological conditions for the formation of N_2O_5 and the relatively low concentration of pCl^-. Generally, the concentration of $ClNO_2$ in autumn is higher than that in spring and summer because higher N_2O_5 and pCl^- concentrations lead to a greater $ClNO_2$ yield. Figures 3i–3l shows the modeled concentrations and spatial distribution differences in $ClNO_2$ between the CL and Base experiments. The monthly average concentration difference reflected the monthly concentration of $ClNO_2$. The increase in the $ClNO_2$ concentration in autumn and winter was primarily due to higher N_2O_5 and pCl^- concentrations, resulting in a greater $ClNO_2$ yield. The increase in $ClNO_2$ concentration in the marine area was limited because of the low concentration of N_2O_5 in that region.

3.2.4. Cl_2—Figures 2m–2p shows the spatial distributions of the monthly mean concentrations of Cl_2 during spring, summer, autumn, and winter in the CL experiment. The spatial patterns of Cl_2 concentrations were relatively similar across different months. In particular, elevated Cl_2 emissions were observed in the central and eastern regions of the YRD, which were attributed to the higher population density, significant industrial activities, widespread use of chlorine-containing disinfectants, and coal combustion in these areas. Conversely, coastal areas exhibit lower Cl_2 concentrations than inland regions, primarily

because of reduced production resulting from heterogeneous reactions of pCl^- with gaseous compounds. When comparing the results of the CL and Base experiments (Figures 3m–3p), the high concentrations of Cl_2 in the central and eastern parts of the YRD can be attributed to three main factors: (a) oceanic Cl emissions, (b) intense anthropogenic emissions, and (c) updated Cl chemistry involving the reaction of pCl^- with O_3 and HOCl.

3.2.5. ClNO—The monthly average concentrations of ClNO in different seasons are shown in Figures 2q–2t. In the Base simulation, the CMAQ5.3.1 mechanism we adopted did not include ClNO as a species; thus, its spatial distribution reflected the variation in ClNO in the simulation. The spatial distribution of ClNO remained consistent across the seasons, although the concentrations were notably higher in autumn and winter than in spring and summer. In the YRD region, the maximum monthly average value of ClNO is 864 pptv in autumn and 667 pptv in winter. ClNO is generated through the heterogeneous interaction between pCl^- and NO_2, hence, its concentration distribution follows a similar pattern to that of pCl^-. Moreover, the concentration of ClNO is lower in marine areas than in inland regions, which may be due to the lower concentrations of NO_2 in the marine environment.

Overall, the predicted concentrations of chlorine-containing compounds exhibited a significant improvement in the CL experiment compared to the Base experiment, and were in better agreement with the available observations. Therefore, the revised model can be effectively used to investigate the impact of chlorine chemistry on air quality in the YRD region.

3.3. Impacts of Reactive Chlorine on Atmospheric Oxidation Capacity

3.3.1. Radicals

3.3.1.1. OH: Figure 4 presents the monthly average distribution of OH in the Base case, as well as the spatial distribution of the difference between the CL and Base cases in different seasons. The concentration of OH varied throughout the year, with the highest monthly average concentration observed in summer, reaching a peak value of 0.39 pptv. Spring exhibited the second highest OH concentration, whereas winter and autumn showed similar concentrations, ranging from 0 to 0.1 pptv. The elevated concentrations of OH in spring and summer can be attributed to the intense solar irradiance and higher ozone levels during these seasons. In a study conducted by Ma et al. (2022), hourly OH concentrations ranging from 0 to 25×10^6 cm^{-3} (equivalent to 0 to 1.016 pptv) and nitrous acid (HONO) concentrations ranging from 0 to 4.4 ppbv were reported in suburban Taizhou, Jiangsu Province, from May to June 2018. In this study, the model-predicted concentrations of OH and HONO for July 2018 were in the ranges of $0–4.5 \times 10^6$ (equivalent to 0–0.18 pptv) and 0–0.7 ppbv, respectively. These predictions were underestimated, potentially due to the absence of certain chemical reactions in the CMAQ model (Zhang et al., 2021).

The addition of chlorine emissions and updates to the chlorine mechanism increased OH generation in the YRD during autumn and winter by 93.4% and 128.6%, respectively. However, in some areas of the YRD during summer, chlorine chemistry inhibits the formation of OH. The impact of chlorine chemistry on OH varies seasonally. In regions with significant anthropogenic chlorine emissions, Cl can enhance OH levels. The influence

of chlorine chemistry on OH is more significant in autumn and winter than in spring and summer because of the higher emissions of chlorine precursors and relatively lower OH concentrations. Cl also promotes the generation of HO_2 by oxidizing additional VOCs, thereby further stimulating OH production. In contrast, during sea breeze events in spring and summer, when the atmospheric levels of NOx and VOCs are lower, the reaction between Cl and O_3 becomes more influential, resulting in reduced O_3 and OH levels. Wang et al. (2019) utilized a global model (GEOS-Chem) and estimated the impact of chlorine emissions on OH over China, ranging from close to zero over land in eastern China to slightly negative over the coast. Wang et al. (2020) employed GEOS-Chem and reported a 6% increase in OH owing to anthropogenic chlorine emissions in China in 2014, with a more pronounced effect in regions with higher anthropogenic chlorine emissions. Q. Y. Li et al. (2020) utilized WRF-Chem to examine the potential impact of halogen chemistry on atmospheric oxidation and air quality in China, revealing that anthropogenic chlorine emissions affect OH by approximately −10%–20% across the country.

3.3.1.2. Cl: In the CL experiment, the concentration of Cl exhibits seasonal variations, with higher levels observed in spring, autumn and winter compared to summer, primarily attributed to the emissions of chlorine precursors (Figure 5). However, the emission inventory of chlorine precursors is subject to certain uncertainties. In this study, we attempted to minimize the discrepancies between the simulated and real emissions by collecting detailed data on the activity levels, emission factors, and geographical coordinates of various chlorine precursor sources. In doing so, we aimed to bridge the gap in Cl emissions from different environmental sources and achieve a more realistic simulation of the spatial distribution of Cl. However, we acknowledge that the uncertainties associated with the emissions inventory may affect the modeling results. The spatial distribution of Cl remained relatively consistent across the seasons. The pCl^- concentration in most areas of the Anhui Province surpasses that of other regions, primarily because of the region's relatively advanced agricultural activities, leading to elevated emissions of pCl^-. The presence of pCl^- facilitates heterogeneous reactions with various substances, thereby promoting the formation and accumulation of Cl_2, $ClNO_2$, and ClNO and consequently increasing the Cl concentration. Additionally, the photolysis of these substances increased the Cl concentration. Conversely, marine regions exhibit lower Cl concentrations than inland areas, mainly because of their lower Cl formation capacity in marine environments. Figure 5 illustrates the changes in Cl concentrations for different months when comparing the CL experiment with the Base case. Following the increase in chlorine emissions and inclusion of the updated chlorine chemistry, the formation of Cl is significantly enhanced during winter and autumn with concentrations reaching 3.9×10^4 molecule cm^{-3} s^{-1} and 3.2×10^4 molecule cm^{-3} s^{-1}, respectively. The increase in Cl concentration is particularly noticeable in the marine areas of southeast Zhejiang province and northeast Jiangsu province compared to other locations. Overall, the increase in Cl concentrations was more prominent in inland areas than in marine regions, highlighting the significant role played by anthropogenic Cl emissions. Hong et al. (2020) employed CMAQ to simulate Cl concentrations in different seasons within the YRD region in 2015, reporting values ranging from 1.0×10^2 molecule cm^{-3} s to 6.9×10^4 molecule cm^{-3} s^{-1}, which are comparable to the simulated Cl concentrations in this study.

3.3.1.3. HO_2: The monthly average distribution of HO_2 in the Base simulation and the impact of chlorine emissions on the monthly concentration distribution of HO_2 in different seasons are shown in Figure 6. The concentration of HO_2 exhibited seasonal variations, with higher levels observed in summer than in other seasons. This can be attributed to the elevated temperatures and increased emissions of VOCs from natural sources. In summer, the concentration of HO_2 in Zhejiang and southern Anhui Provinces surpassed that in other regions within the YRD and reached levels greater than 12 pptv. This notable occurrence can be primarily attributed to the substantial VOC emissions released by trees and vegetation in the Zhejiang and Anhui regions. As these VOCs are oxidized by various oxidants, the concentration of HO_2 increases significantly. In spring, the spatial distribution of HO_2 followed a similar pattern to that in summer but with lower concentrations. In contrast, during winter and autumn, the monthly average concentration of HO_2 in the YRD region was lower, ranging from 0 to 5 pptv.

The influence of chlorine on HO_2 in the YRD was more prominent during winter and autumn and weaker in summer than in spring. There are two reasons for the apparent increase in HO_2 in most areas of YRD during autumn and winter. First, the emissions of chlorine precursors were higher during these seasons, leading to an increase in the Cl concentration. Consequently, additional oxidation of VOCs is promoted, resulting in the formation of HO_2. However, the relatively low concentration of HO_2 in the Base case simulation during autumn and winter amplified the impact of a small increase in OH, resulting in a substantial relative change. In summer, slight decreases in HO_2 were observed in parts of Zhejiang and southern Anhui provinces. This is primarily due to the dominant role of OH during summer and the competitive reaction between Cl and OH and VOCs, which inhibits the formation of HO_2.

3.3.1.4. RO_2: Figure 7 displays the monthly average distribution of RO_2 in the Base experiment, as well as the spatial distribution of the RO_2 difference between the CL and Base experiments across different months. The spatial variation of RO_2 followed a pattern similar to that of HO_2. In summer, Zhejiang Province exhibited a high monthly average concentration of RO_2, reaching 73.3 pptv. In contrast, monthly average concentration of RO_2 is lower in autumn and winter than in spring and summer. The introduction of chlorine emissions had a notable impact on the concentration of RO_2 in the YRD during winter and autumn. In regions with high chlorine emissions, the concentration of RO_2 increased by up to 190.8% and 213.0% in autumn and winter, respectively. This increase was primarily attributed to the oxidation of VOCs by Cl and the subsequent formation of RO_2. However, the impact on monthly average concentration of RO_2 in spring and summer in the YRD region was minimal. This can be attributed to the high levels of OH in the Base experiment during spring and summer as well as the relatively smaller influence of Cl compared to autumn and winter.

3.3.1.5. NO_3: Figure 8 illustrates the monthly average distribution of NO_3 in the Base case, along with the influence of chlorine chemistry on the monthly average concentration of NO_3 in different seasons. The monthly average NO_3 concentrations in the YRD region exhibited slight variations across different months. Notably, the concentration of NO_3 in the

marine region surpassed that in the inland region. This disparity can be attributed to lower levels of VOCs and reduced deposition velocity in the marine area. Furthermore, the NO_3 concentration in the marine region tends to be higher in summer and autumn than in spring and winter. The addition of chlorine emissions and updated chlorine chemistry primarily enhanced the formation of NO_3 in the polluted regions of the YRD. In polluted areas, Cl promotes higher levels of O_3, consequently increasing the formation of NO_3 through the reactions between NO_2 and O_3. However, in cleaner regions, such as the ocean, Cl chemistry reduces the levels of O_3, thereby decreasing the concentration of NO_3.

3.3.2. AOC

3.3.2.1. Spatial Distribution: Figure 9 shows the monthly average spatial distribution of AOC in the Base case, as well as the changes in AOC between the CL and Base experiments in different months in the YRD region. The spatial concentration patterns of the monthly average AOC exhibit similarity during winter and autumn, with AOC levels ranging from 2.0 to 8.0 × 10^6 molecule·cm^{-3} s^{-1}. In contrast, AOC levels in spring and summer are higher than those in winter and autumn, ranging from 10^6 to 10^7 molecular·cm^{-3} s^{-1}. The pronounced increase in AOC during summer primarily stems from intensified sunlight, which leads to higher concentrations of OH and O_3. These oxidants react with VOCs, thereby augmenting the AOC levels. In comparison, the concentrations of AOC in the marine areas were lower than those in the inland areas during the different months. This discrepancy mainly arises from the diminished levels due to the lower concentrations of oxidants (OH and O_3) and reactants (CO and VOCs) in the marine environment.

The addition of chlorine (Figure 9) enhanced the AOC. The impact of chlorine emissions on AOC varied across different seasons, with a greater influence observed in winter than in autumn. In spring, the impact is higher than that in summer due to initially low levels of AOC in the Base case, resulting in a substantial relative change rate when the AOC experiences a slight increase. Cl, as a promoter of VOC oxidation, plays a crucial role in enhancing AOC during autumn and winter. The introduction of chlorine chemistry significantly boosted AOC levels in Jiangsu and Anhui Provinces during all seasons, with maximum increases of 202.9%, 108.2%, 280.0%, and 404.2% in spring, summer, autumn, and winter, respectively. These regions, which are characterized by higher emissions of chlorine precursors, experience a more pronounced enhancement of atmospheric oxidation. The considerable impact of chlorine emissions on AOC highlights the need to consider chlorine precursor emissions in air quality models to accurately assess atmospheric oxidation processes. Additionally, our findings indicate that the influence of chlorine chemistry on air quality is more pronounced during summer and winter. Specifically, the impact of chlorine chemistry on AOC was considerably greater during winter than during summer. Moreover, Cl assume a more significant role in winter atmospheric chemistry.

3.3.2.2. Temporal Distribution: Figure 10 shows the average hourly AOC during different seasons in the YRD region for both the Base and CL experiments. The AOC values during the daytime were significantly higher than those during the nighttime because of the enhanced rates of atmospheric chemical reactions and the formation of oxidants facilitated by sunlight. In various months, the daytime AOC was one to two orders of

magnitude greater than the nighttime AOC, which was primarily attributed to the substantial contribution of OH to the AOC during daylight hours. In the Base case, OH accounted for 92.9%, 94.2%, 86.7%, and 88.5% of the AOC in the spring, summer, autumn, and winter, respectively. The contributions of O_3 to AOC were 5.0%, 3.7%, 10.2%, and 9.7% in spring, summer, autumn, and winter, respectively. NO_3 contributed less than 4% in all seasons.

In the CL experiment, following the increase in chlorine emissions and the updating of chlorine chemistry, the contributions of Cl to AOC were 5.2%, 2.8%, 9.7%, and 11.3% in spring, summer, autumn, and winter, respectively. The inclusion of chlorine chemistry in the CL experiment increased its contribution to AOC by 21.3%, 8.7%, 43.3%, and 58.7% in spring, summer, autumn, and winter, respectively. Compared to the Base case, the promotional effect of OH on the AOC in spring, summer, autumn, and winter was amplified by 15.6%, 5.7%, 32.3%, and 44.4%, respectively. The influence of chlorine chemistry on O_3 modified AOC by −2.4%, −11.2%, 2.4%, and 6.1% in spring, summer, autumn, and winter, respectively.

Chlorine chemistry exhibited contrasting effects on daytime (6:00–17:00) and nighttime (18:00–5:00) AOC. The introduction of chlorine emissions resulted in a reduction in nighttime AOC by diminishing the contributions of OH and O_3 to AOC in different months. This reduction can be attributed to the heterogeneous reactions of OH and O_3 with pCl^-, which consume atmospheric oxidants and limit their reactions with VOCs. Conversely, the addition of chlorine emissions led to an increase in daytime AOC, with the most significant enhancement observed in winter and autumn. Chlorine promotes the contribution of OH to AOC during the daytime, primarily through the promotion of VOCs oxidation, which subsequently enhances the formation of OH.

3.4. Impacts of Chlorine Chemistry on O_3

3.4.1. Spatial Distribution—Figure 11 depicts the monthly average distribution of MDA8 O_3 in the Base case and illustrates the impact of chlorine chemistry ((CL-Base)/Base) on the spatial distribution of MDA8 O_3 in different months. During spring and summer, the monthly average concentration of MDA8 O_3 tended to be higher than that during winter and autumn. The primary factor behind this phenomenon is the higher temperatures typically experienced during spring and summer as opposed to autumn and winter. These elevated temperatures create meteorological conditions that are favorable for the formation of O_3. The influence of chlorine emissions on the monthly average concentration of MDA8 O_3 in the YRD varied across seasons, with more pronounced enhancements observed in autumn and winter than in other seasons. The average monthly impacts of chlorine chemistry on MDA8 O_3 in the simulated area (YRD and marine area) are as follows: −0.6% (−0.3 ppbv) in spring, −0.2% (−0.1 ppbv) in summer, 3.2% (1.2 ppbv) in autumn and 5.6% (2.2 ppbv) in winter. The maximum percentage enhancements in chlorine emissions from MDA8 O_3 in the YRD region were as follows: 8.4% in spring, 5.8% in summer, 16.9% in autumn, and 18.1% in winter. The corresponding maximum absolute enhancements are 4.6, 4.1, 7.0, and 6.7 ppbv, respectively. Notably, chlorine emissions reduced the formation of MDA8 O_3 in summer, with the largest reduction observed at 3.3%, owing to the reaction of Cl with O_3. Hong et al. (2020) conducted

a study that supported the influence of anthropogenic chlorine emissions on the average concentration of MDA8 O_3 in eastern China. The study revealed that the impact of these emissions ranged from −0.2 to 4.9 ppbv in July, with a more substantial effect observed during autumn and winter than during spring and summer. Remarkably, their research demonstrated that chlorine chemistry, considering emissions such as HCl and Cl_2 from coal combustion and waste incineration as well as pCl^- from conventional pollutants, can both promote and inhibit O_3 formation. Specifically, in July, our findings suggest that chlorine chemistry may have a more noticeable effect on suppressing O_3 when considering the complete chlorine emissions and the associated chemistry.

3.4.2. Temporal Distribution—Figure 12 illustrates the temporal variation in the impact of chlorine emissions on O_3 in Hangzhou, Hefei, Nanjing, and Shanghai during the different seasons. The hourly impacts of chlorine chemistry on O_3 in these major cities range between −0.3 and 3.3 ppbv in spring, −0.4 to 4.3 ppbv in summer, −0.2 to 7.2 ppbv in autumn, and 0.2–6.3 ppbv in winter. The enhancement in chlorine emissions by O_3 was more significant in autumn and winter than in spring and summer. The maximum hourly increase in O_3 was observed in Hangzhou during autumn (6.3 ppbv) and Nanjing during winter (7.2 ppbv). In Shanghai, the maximum hourly increase in O_3 occurred in spring (3.3 ppbv), and in Nanjing, it occurred in summer (4.3 ppbv). Furthermore, chlorine emissions have distinct seasonal impacts on O_3 between 10:00 and 11:00 in autumn and winter and at 8:00 in spring and summer. This is because Cl precursors accumulate at night and generate a substantial amount of Cl in the early morning following sunrise, thereby promoting VOC oxidation and leading to the formation of O_3.

3.5. Impacts of Chlorine Chemistry on $PM_{2.5}$ and Its Chemical Components

3.5.1. $PM_{2.5}$—Figure 13 shows the monthly average distribution of $PM_{2.5}$, and the impact of chlorine emissions on $PM_{2.5}$ during the different seasons. The monthly average concentration of $PM_{2.5}$ in the YRD region, exhibited slight variation across different seasons, typically ranging from 15 to 60 $\mu g/m^3$. The addition of chlorine emissions had different effects on the monthly average $PM_{2.5}$, in different seasons. In spring and summer, the addition of chlorine inhibits the formation of $PM_{2.5}$ in certain parts of the YRD region. The negative impact of chlorine emissions on $PM_{2.5}$ is more pronounced in spring than in summer, with a potential decrease of up to 1 $\mu g/m^3$ in the monthly average $PM_{2.5}$ concentration in spring than in summer. Conversely, chlorine emissions promoted the formation of $PM_{2.5}$ in most areas of the YRD region during winter and autumn, resulting in more significant increases of 11.1 and 13.2 $\mu g/m^3$, respectively. The influence of chlorine emissions on $PM_{2.5}$ primarily occurs through the formation of its constituents such as nitrate, sulfate, and ammonium. A previous study by Wang et al. (2020), using the GEOS-Chem model, demonstrated that chlorine has the potential to increase annual mean $PM_{2.5}$ by up to 3.2 $\mu g/m^3$. Similarly, J. Y. Li et al. (2021) and Zhang et al. (2020) incorporated the multiphase chemistry of chlorine into the CMAQ model and reported that chlorine emissions can enhance $PM_{2.5}$ by 2%–6% in the YRD region during spring.

3.5.2. Nitrate—Figure 14 illustrates the monthly average distribution of nitrate ($NO_3^-{}_{2.5}$) in the Base case during different seasons. The concentration of $NO_3^-{}_{2.5}$ exhibits variations

across different seasons, with higher levels observed during autumn and winter than in spring and summer. This pattern can be attributed to lower temperatures during autumn and winter, which promoted the formation of N_2O_5 and nitrate through the heterogeneous hydrolysis of N_2O_5. The middle region of the YRD showed higher nitrate concentrations than other areas. In contrast, most regions in Zhejiang exhibited relatively low levels of nitrate, primarily because of lower NO_x emissions in that particular region.

In the presence of Cl emissions, the formation of $NO_3^-{}_{2.5}$ is increased in most areas during winter and autumn, with concentration enhancements of 4.1 μg/m^3 and 3.9 μg/m^3, respectively. The emission of chlorine precursors, which is higher during autumn and winter, leads to elevated Cl levels. Cl promotes the formation of OH and O_3, accelerating the conversion of NO_x to $NO_3^-{}_{2.5}$. Additionally, some heterogeneous reactions contribute to the formation of $NO_3^-{}_{2.5}$. The influence of chlorine emissions on $NO_3^-{}_{2.5}$ formation in the YRD region during spring and summer is relatively small, with ranges of −0.8 μg/m^3 to 2.5 μg/m^3 and −0.3 μg/m^3 to 1.8 μg/m^3, respectively. In fact, chlorine emissions inhibit the formation of $NO_3^-{}_{2.5}$ during spring and summer, with maximum inhibitory effects of 0.8 μg/m^3 and 0.3 μg/m^3, respectively. The inhibitory effect of chlorine emissions on $NO_3^-{}_{2.5}$ is more pronounced in spring compared to summer. This inhibition was primarily attributed to the heterogeneous reaction of N_2O_5 with particulate chloride, which reduced the formation of HNO_3 and subsequently lowered the production of $NO_3^-{}_{2.5}$ (Su et al., 2017). These findings align with those of previous studies by Zhang et al. (2020), who reported significant reductions in NO_3^- concentrations in Southwest China in November due to chlorine chemistry. The reduction of monthly mean NO_3^- in the YRD region by chlorine emissions ranged from −1 to 0 μg/m^3, which is consistent with the results of this study. J. Y. Li et al. (2021) also observed different effects of chlorine emissions on $NO_3^-{}_{2.5}$ in different regions, with both promoting and inhibiting effects.

3.5.3. Sulfate—Figure 15 presents the monthly average distribution of sulfate ($SO_4^{2-}{}_{2.5}$) in the Base experiment along with the impact of chlorine emissions (CL-Base) on the monthly average $SO_4^{2-}{}_{2.5}$ during different seasons. The spatial distribution of $SO_4^{2-}{}_{2.5}$ remains consistent across different seasons. Notably, the central part of the YRD exhibited relatively high monthly average concentrations of $SO_4^{2-}{}_{2.5}$, closely associated with contributions from industrial processes and combustion sources. When comparing the Base experiment with the addition of chlorine emissions, the monthly average impacts of chlorine chemistry on $SO_4^{2-}{}_{2.5}$ within the simulation area are as follows:−0.05 μg/m^3 in spring, −0.02 μg/m^3 in summer, 0.04 μg/m^3 in autumn, and 0.06 μg/m^3 in winter, respectively. Consequently, the inclusion of chlorine emissions has minimal effects on $SO_4^{2-}{}_{2.5}$ within the YRD region, with monthly average variations ranging from −1.29 to 0.39 μg/m^3. Wang et al. (2020) also reported negligible effects of anthropogenic chlorine emissions on $SO_4^{2-}{}_{2.5}$ concentrations in China, with values below 0.1 μg/m^3. In summary, the overall, the influence of chlorine emissions on $SO_4^{2-}{}_{2.5}$ is deemed insignificant.

3.5.4. Ammonia—Figure 16 shows the monthly average distribution of ammonia ($NH_4^+{}_{2.5}$) in the Base experiment as well as the difference between the CL and Base

experiments across different seasons. The spatial distribution of $NH_4^+{}_{2.5}$ was similarity to that of $NO_3^-{}_{2.5}$ throughout the various seasons.

The impact of chlorine emissions on the monthly average concentration distribution of $NH_4^+{}_{2.5}$ is akin to its effect on $NO_3^-{}_{2.5}$. Notably, the promoting effect of Cl emissions on $NH_4^+{}_{2.5}$ was more pronounced during autumn and winter than during spring and summer. Moreover, chlorine emissions exhibited twofold effects, promoting and inhibiting $NH_4^+{}_{2.5}$ formation in different regions and seasons. The presence of particulate chloride contributes to a decrease in the heterogeneous formation of nitric acid. Consequently, the reaction between nitric acid and NH_3 diminished, leading to a reduction in the concentration of $NH_4^+{}_{2.5}$. However, in the winter and autumn seasons, chlorine emissions foster the formation of $NH_4^+{}_{2.5}$ in the YRD region, resulting increases of up to 2.6 and 2.7 $\mu g/m^3$, respectively. These enhancements can be attributed to the increased concentration of NO_x, which is then converted into nitric acid through the additional OH generated from chemical reactions. Subsequently, the reaction between nitric acid and NH_3 led to the formation of NH_4NO_3, thus increasing the concentration of $NH_4^+{}_{2.5}$. The impact of chlorine emissions on $NH_4^+{}_{2.5}$ in different regions of the YRD region during different months varies significantly and is primarily dependent on the concentration of Cl (presumably referring to the concentration of Cl).

3.5.5. Organic Carbon—Figure 17 illustrates the monthly average concentration distribution of organic carbon ($OC_{2.5}$) in $PM_{2.5}$ during different seasons. The concentration of $OC_{2.5}$ remains relatively similar across the different seasons, with a noteworthy exception in autumn when significantly higher levels were observed in the Anhui region. Comparing the Base experiment with the inclusion of chlorine emissions, it was found that chlorine emissions contributed to the enhancement of the monthly average $OC_{2.5}$ across the modeling domain. Specifically, in spring, summer, autumn, and winter, the average increases were 0.09, 0.05, 0.36, and 0.44 $\mu gC/m^3$, respectively. Furthermore, within the YRD region, chlorine emissions lead to an elevation in the monthly maximum $OC_{2.5}$ concentrations of 0.7, 1.0, 2.0, and 1.5 $\mu gC/m^3$ during spring, summer, autumn, and winter, respectively. The stronger impact of chlorine emissions on $OC_{2.5}$ during autumn and winter, compared to spring and summer, can be attributed to the higher concentration of Cl during the former seasons. This elevated concentration of Cl promotes the formation of OH, which, in turn, facilitates additional oxidation of VOCs. Consequently, the formation of secondary organic aerosols increases, leading to higher concentrations of $OC_{2.5}$.

3.6. Comparisons With Previous Studies

Previous studies have explored the influence of chlorine chemistry on air quality using various models and emissions, as summarized in Table 3. The most prominent among these models are Chemical Transport Models, such as CMAQ, CAMx, and WRF-Chem. These models have been widely employed to investigate the effects of chlorine emissions and chemistry on O_3, $PM_{2.5}$, and their chemical components. In our study, we have taken a more comprehensive approach by considering a broader range of chlorine precursors, including Cl_2, HOCl, HCl, and pCl^-. To assess the impacts of chlorine emissions on different pollutants across the YRD region during various seasons, we utilized the WRF-CMAQ

modeling system with updated chlorine chemistry. This integrated modeling system allowed for a more detailed examination of the effects of chlorine emissions on air quality within the study area.

Sarwar et al. (2014) used the CMAQ model to investigate the influence of chlorine emissions in the Northern Hemisphere. Their findings revealed that the impact of chlorine emissions was more substantial during the winter than during the summer. Specifically, the impact on the MDA8 O_3 concentration was 7 ppbv in winter and 1.6 ppbv in summer. Moreover, the impact on OH concentration was 3.5% in winter and 0.3% in summer. In studies conducted in China, it was observed that chlorine emissions have varying effects on 1 h O_3, monthly average MDA8 O_3, and OH concentrations, as summarized in Table 3. The range of the influence of chlorine emissions on these parameters in China is reported to be 0–34.3 ppbv for 1 h O_3, −8 4.9 ppbv for monthly average MDA8 O_3, and 0%–101.4% for OH concentrations. In our study, we examined the impact of chlorine emissions on 1 h O_3, monthly average MDA 8 O_3, and OH concentrations, resulting in ranges of −0.8–12.0 ppbv, −0.7–7.0 ppbv, and −5.9%–128.6%, respectively. Consistent with the findings of Hong et al. (2020), the promotional effect of chlorine chemistry on O_3 was significantly greater in autumn and winter than in spring and summer. In addition, our study considered the impact of chlorine emissions on AOC, which showed a similar effect on O_3. Previous studies have also explored impact of chlorine emissions on monthly average nitrate and $PM_{2.5}$ concentrations, ranging from −2.5 to 13.5 μg/m^3 and 3.2 to 7.5 μg/m^3, respectively. In our study, the impact on these two species ranged from—0.8to 4.1 μg/m^3 and −1.0 to 13.2 μg/m^3, respectively. These effects were comparable to those reported in previous studies.

Most studies have indicated that chlorine emissions promote the formation of O_3. However, in recent years, studies have suggested that chlorine emissions may inhibit O_3 formation (Zhang et al., 2020; Wang et al., 2019). In line with these findings, our study highlights that chlorine emissions have the dual capacity to promote and limit the formation of O_3 and $PM_{2.5}$ in different seasons and areas. Specifically, our results demonstrate that chlorine emissions play a significant role in promoting the formation of O_3 and $PM_{2.5}$. This effect was observed across various seasons and areas. Notably, the promotional effect is more pronounced in autumn and winter than in spring and summer. However, our study also reveals that the potential for chlorine emissions limits the formation of O_3 and $PM_{2.5}$. These findings highlight the complex and nuanced nature of the relationship between chlorine emissions and air pollutants, with both promoting and inhibitory effects observed under different scenarios.

4. Conclusions

In this study, we investigated the impact of anthropogenic and sea salt chlorine emissions on air quality. We utilized the WRF-CMAQ model, incorporating 13 updated gases and eight heterogeneous chlorine chemistries, to assess the influence of chlorine emissions on air quality in different seasons over the YRD region. Two simulations were conducted to examine these effects. By incorporating the 21 additional chemical reactions to the current CB6r3_ae7 mechanisms coupled within CMAQ, the Mean Bias for predicting O_3 and $PM_{2.5}$ are overall reduced. The introduction of chlorine emissions led to enhancements in AOC,

with regions characterized by higher chlorine emissions and substantial relative changes in AOC. Notably, the relative changes in AOC were more pronounced during winter and autumn, whereas smaller changes were observed during spring and summer. The impact of chlorine emissions is more significant in autumn and winter than in spring and summer. Temporal analysis of AOC revealed that chlorine emissions significantly increased AOC concentrations during daytime hours. Cl, in particular, contributes significantly to AOC during daytime, with a significant contribution of 11.3% in winter and 9.7% in autumn. The contribution of Cl to AOC through the promotion of OH increased by 15.6%, 5.7%, 32.3%, and 44.4% during the spring, summer, autumn, and winter, respectively. The diurnal impacts of chlorine emissions significantly enhance OH concentrations, thereby augmenting the oxidative capacity through the additional oxidation of VOCs. While chlorine emissions have a slight reduction effect on nighttime AOC, primarily attributable to the depletion of O_3 and OH by Cl, consequently diminishing the contributions of O_3 and OH to AOC. Furthermore, the study finds that chlorine emissions had a greater enhancing effect on OH, HO_2, and O_3 in the YRD region during winter and autumn than during spring and summer. Overall, chlorine emissions exerted a more substantial promoting influence on free radicals and O_3 during autumn and winter.

The influence of chlorine emissions on $PM_{2.5}$ and its components varies across seasons in the YRD region. Notably, chlorine emissions have minimal impact on the formation of $PM_{2.5}$ during spring and summer while they significantly enhance the formation of $PM_{2.5}$ during autumn and winter, with average maximum monthly increases of 13.2 $\mu g/m^3$ and 11.1 $\mu g/m^3$ have been observed as a result of chlorine emissions in specific areas of the YRD region. Chlorine chemistry played a notable role in influencing the composition of $PM_{2.5}$, particularly in relation to $NO_3^-{}_{2.5}$, $NH_4^+{}_{2.5}$, and $OC_{2.5}$. The effects of these components are significant. However, chlorine emissions had a relatively small impact on $SO_4^{2-}{}_{2.5}$, another component of $PM_{2.5}$.

This is the first study to introduce a disinfectant source into the chlorine precursor emission inventory for the YRD region. The chemical reaction mechanism of chlorine synthesized in previous studies was incorporated into the CMAQ model to investigate the effects of chlorine chemistry on various parameters during different seasons in the YRD. However, uncertainties are associated with the uptake coefficients used for heterogeneous reactions of pCl^-. These uncertainties stem from limited observational data on chlorine-containing substances in the YRD and China. Future field and laboratory studies are recommended to improve the understanding of these uncertainties. These studies can help refine the uptake coefficients and provide measurements of chlorine-containing substances in YRD and China. By incorporating these improved coefficients and measurements into the models, we further enhanced our assessment of the impact of chlorine emissions on air quality.

Supplementary Material

Refer to Web version on PubMed Central for supplementary material.

Acknowledgments

This research is supported by the National Natural Science Foundation of China under Grant 42075144. The CSIC team is supported by the European Research Council Executive Agency under the European Union's Horizon 2020 Research and Innovation Programme (Project ERC-2016- COG 726349 CLIMAHAL). The HKPolyU team is supported by the Hong Kong Research Grants Council (Project T24-504/17-N). This work is supported by Shanghai Technical Service Center of Science and Engineering Computing, Shanghai University.

Data Availability Statement

The observational data used and demonstrated in this study are collected from related references, which have been listed in the manuscript as well as the references. The chlorine emission inventory and updated chlorine chemical mechanism code file utilized in this research can be available from https://doi.org/10.5281/zenodo.7997238 (Yi et al., 2023).

References

Abbatt JPD, & Waschewsky GCG (1998). Heterogeneous interactions of HOBr, HNO_3, O_3, and NO_2 with deliquescent NaCl aerosols at room temperature. Journal of Physical Chemistry, 102(21), 3719–3725. 10.1021/jp980932d

Aschmann SM, & Atkinson R (1995). Rate constants for the gas-phase reactions of alkanes with Cl atoms at 296 ± 2 K. International Journal of Chemical Kinetics, 27(6), 613–622. 10.1002/kin.550271206

Bertram TH, & Thornton JA (2009). Toward a general parameterization of N_2O_5 reactivity on aqueous particles: The competing effects of particle liquid water, nitrate and chloride. Atmospheric Chemistry and Physics Discussions, 9, 191–198. 10.5194/acp-9-8351-2009

Chang S, & Allen D (2006). Atmospheric chlorine chemistry in southeast Texas: Impacts on ozone formation and control. Environmental Science and Technology, 40(1), 251–262. 10.1021/es050787z [PubMed: 16433359]

Chang S, Mcdonald-Buller E, Kimura Y, Yarwood G, Neece J, Russell M, et al. (2002). Sensitivity of urban ozone formation to chlorine emission estimates. Atmospheric Environment, 36(32), 4991–5003. 10.1016/S1352-2310(02)00573-3

Chang S, Tanaka P, McDonald-Buller E, & Allen DT (2001). Emission inventory for atomic chlorine precursors in Southeast Texas Report on Contract 9880077600–18 between the University of Texas and the Texas Natural Resource Conservation Commission. Center for Energy and Environmental Resources, University of Texas.

Chen QJ, Xia M, Peng X, Yu C, Sun P, Li YY, et al. (2022). Large daytime molecular chlorine missing source at a suburban site in East China. Journal of Geophysical Research: Atmospheres, 127(4), e2021JD035796. 10.1029/2021JD035796

Cho SY, Park HY, Son JS, & Chang LS (2021). Development of the global to mesoscale air quality forecast and analysis system (GMAF) and its application to $PM_{2.5}$ forecast in Korea. Atmosphere, 12(3), 411. 10.3390/atmos12030411

Choi MS, Qiu X, Zhang J, Wang S, Li X, Sun Y, et al. (2020). Study of secondary organic aerosol formation from chlorine radical-initiated oxidation of volatile organic compounds in a polluted atmosphere using a 3D chemical transport model. Environmental Science and Technology, 54(21), 13409–13418. 10.1021/acs.est.0c02958 [PubMed: 33074656]

Dai J, Liu Y, Wang P, Fu X, Xia M, & Wang T (2020). The impact of sea-salt chloride on ozone through heterogeneous reaction with N_2O_5 in a coastal region of south China. Atmospheric Environment, 236, 117604. 10.1016/j.atmosenv.2020.117604

Deiber G, Ch G, Calvé SL, Schweitzer F, & Ph M (2004). Uptake study of $ClONO_2$ and $BrONO_2$ by Halide containing droplets. Atmospheric Chemistry and Physics, 4(5), 1291–1299. 10.5194/acp-4-1291-2004

Fu X, Wang T, Wang SX, Zhang L, Cai SY, Xing J, & Hao JM (2018). Anthropogenic emissions of hydrogen chloride and fine particulate chloride in China. Environmental Science and Technology, 52(3), 1644–1654. 10.1021/acs.est.7b05030 [PubMed: 29376646]

Gantt B, Kelly JT, & Bash JO (2015). Updating sea spray aerosol emissions in the Community Multiscale Air Quality (CMAQ) model version 5.0.2. Geoscientific Model Development, 8(11), 3733–3746. 10.5194/gmd-8-3733-2015

Guenther A, Karl T, Harley P, Wiedinmyer C, Palmer ZY, & Geron C (2006). Estimates of global terrestrial isoprene emissions using MEGAN (model of emissions of gases and aerosols from nature). Atmospheric Chemistry and Physics, 6(11), 3181–3210. 10.5194/acp-6-3181-2006

Haskins JD, Lee BH, Lopez-Hilifiker FD, Peng Q, Jaeglé L, Reeves JM, et al. (2019). Observational constraints on the formation of Cl_2 from the reactive uptake of $ClNO_2$ on aerosols in the polluted marine boundary layer. Journal of Geophysical Research: Atmospheres, 124(15), 8851–8869. 10.1029/2019JD030627

Haskins JD, Lopez-Hilfiker FD, Lee BH, Shah V, Wolfe GM, DiGangi J, et al. (2019). Anthropogenic control over wintertime oxidation of atmospheric pollutants. Geophysical Research Letters, 46(24), 14826–14835. 10.1029/2019GL085498 [PubMed: 33012881]

Hong YY, Liu YM, Chen X, Qi FD, Chen CE, Fan Q, et al. (2020). The role of anthropogenic chlorine emission in surface ozone formation during different seasons over eastern China. Science of the Total Environment, 723, 137697. 10.1016/j.scitotenv.2020.137697 [PubMed: 32392687]

Huang L, Wang Q, Wang YJ, Emery C, Zhu AS, Zhu YH, et al. (2021). Simulation of secondary organic aerosol over the Yangtze River Delta region: The impacts from the emissions of intermediate volatility organic compounds and the SOA modeling framework. Atmospheric Environment, 246, 118079. 10.1016/j.atmosenv.2020.118079

Huang L, Zhu YH, Zhai HH, Xue SH, Zhu TY, Shao Y, et al. (2021). Recommendations on benchmarks for numerical air quality model applications in China – Part 1: $PM_{2.5}$ and chemical species. Atmospheric Chemistry and Physics, 21(4), 2725–2743. 10.5194/acp-21-2725-2021

Il'in SD, Selikhanovich VV, Gershenzon YM, & Rozenshtein VB (1991). Study of heterogeneous ozone loss on materials typical of atmospheric aerosol species. Soviet Journal of Chemical Physics, 8, 1858–1880.

Keene W, Khalil MAK, Erickson D, McCulloch A, Graedel TE, Lobert JM, et al. (1999). Composite global emissions of reactive chlorine from anthropogenic and natural sources: Reactive Chlorine Emissions Inventory. Journal of Geophysical Research, 104(D7), 8429–8440. 10.1029/1998JD100084

Knipping EM, & Dabdub D (2003). Impact of chlorine emissions from sea-salt aerosol on coastal urban ozone. Environmental Science and Technology, 37(2), 275–284. 10.1021/es025793z [PubMed: 12564898]

Lawler M, Sander R, Carpenter L, Lee J, Von Glasow R, Sommariva R, & Saltzman E (2011). HOCl and Cl_2 observations in marine air. Atmospheric Chemistry and Physics Discussions, 11(15), 7617–7628. 10.5194/acp-11-7617-2011

Li FB, Huang DD, Nie W, Tham YJ, Lou SR, Li YY, et al. (2023). Observation of nitrogen oxide-influenced chlorine chemistry and source analysis of Cl_2 in the Yangtze River Delta, China. Atmospheric Environment, 306, 119829. 10.1016/j.atmosenv.2023.119829

Li JY, Zhang N, Wang P, Choi M, Ying Q, Guo S, et al. (2021). Impacts of chlorine chemistry and anthropogenic emissions on secondary pollutants in the Yangtze river delta region. Environmental Pollution, 287, 117624. 10.1016/j.envpol.2021.117624 [PubMed: 34192645]

Li QY, Badia A, Wang T, Sarwar G, Fu X, Zhang L, et al. (2020). Potential effect of halogens on atmospheric oxidation and air quality in China. Journal of Geophysical Research: Atmospheres, 125(9), e2019JD032058. 10.1029/2019JD032058

Li Y, Carlton AG, & Shiraiwa M (2021). Diurnal and seasonal variations in the phase state of secondary organic aerosol material over the contiguous us simulated in CMAQ. ACS Earth and Space Chemistry, 5(8), 1971–1982. 10.1021/acsearthspacechem.1c00094

Li Q, Zhang L, Wang T, Tham YJ, Ahmadov R, Xue LK, et al. (2016). Impacts of heterogeneous uptake of dinitrogen pentoxide and chlorine activation on ozone and reactive nitrogen partitioning:

Improvement and application of the WRF-chem model in southern China. Atmospheric Chemistry and Physics, 16(23), 14875–14890. 10.5194/acp-16-14875-2016

Liu XX, Qu H, Huey LG, Wang YH, Sjostedt S, Zeng LM, et al. (2017). High levels of daytime molecular chlorine and nitryl chloride at a rural site on the North China Plain. Environmental Science and Technology, 51(17), 9588–9595. 10.1021/acs.est.7b03039 [PubMed: 28806070]

Liu YM, Fan Q, Chen XY, Zhao J, Ling ZH, Hong YY, et al. (2018). Modeling the impact of chlorine emissions from coal combustion and prescribed waste incineration on tropospheric ozone formation in China. Atmospheric Chemistry and Physics, 18(4), 2709–2724. 10.5194/acp-18-2709-2018

Ma XF, Tan ZF, Lu KD, Yang XP, Chen XR, Wang HC, et al. (2022). OH and HO_2 radical chemistry at a suburban site during the EXPLORE-YRD campaign in 2018. Atmospheric Chemistry and Physics, 22(10), 7005–7028. 10.5194/acp-22-7005-2022

Millero FJ (2013). Chemical oceanography (4th ed.). CRC Press. 10.1201/b14753

Pratte P, & Rossi MJ (2006). The heterogeneous kinetics of HOBr and HOCl on acidified sea salt and model aerosol at 40–90% relative humidity and ambient temperature. Physical Chemistry Chemical Physics Pccp, 8(34), 3988–4001. 10.1039/B604321F [PubMed: 17028689]

Qiu XH, Ying Q, Wang S, Duan L, Zhao J, Xing J, et al. (2019a). Modeling the impact of heterogeneous reactions of chlorine on summertime nitrate formation in Beijing, China. Atmospheric Chemistry and Physics, 19(10), 6737–6747. 10.5194/acp-19-6737-2019

Qiu XH, Ying Q, Wang SX, Duan L, Wang YH, Lu KD, et al. (2019b). Significant impact of heterogeneous reactions of reactive chlorine species on summertime atmospheric ozone and free-radical formation in north China. Science of the Total Environment, 693, 133580. 10.1016/j.scitotenv.2019.133580 [PubMed: 31376754]

Quack M, & Willeke M (2010). Absolute and relative rate constants for the reactions of hydroxyl radicals and chlorine atoms with a series of aliphatic alcohols and ethers at 298 K. International Journal of Chemical Kinetics, 22, 1111–1126. 10.1002/kin.550221102

Roberts JM, Osthoff HD, Brown SS, & Ravishankara A (2008). N_2O_5 oxidizes chloride to Cl_2 in acidic atmospheric aerosol. Science, 321(5892), 1059. 10.1126/science.1158777 [PubMed: 18599742]

Roberts JM, Osthoff HD, Brown SS, Ravishankara A, Coffman D, Quinn P, & Bates T (2009). Laboratory studies of products of N_2O_5 uptake on Cl^- containing substrates. Geophysical Research Letters, 36(20), L20808. 10.1029/2009GL040448

Rudich Y, Talukdar RK, Ravishankara A, & Fox R (1996). Reactive uptake of NO_3 on pure water and ionic solutions. Journal of Geophysical Research, 101(D15), 21023–21031. 10.1029/96JD01844

Sarwar G, & Bhave PV (2007). Modeling the effect of chlorine emissions on ozone levels over the eastern United States. Journal of Applied Meteorology and Climatology, 46(7), 1009–1019. 10.1175/JAM2519.1

Sarwar G, Simon H, Bhave P, & Yarwood G (2012). Examining the impact of heterogeneous nitryl chloride production on air quality across the United States. Atmospheric Chemistry and Physics Discussions, 12(14), 6455–6473. 10.5194/acp-12-6455-2012

Sarwar G, Simon H, Xing J, & Mathur R (2014). Importance of tropospheric $ClNO_2$ chemistry across the northern hemisphere. Geophysical Research Letters, 41(11), 4050–4058. 10.1002/2014GL059962

Saul TD, Tolocka MP, & Johnston MV (2006). Reactive uptake of nitric acid onto sodium chloride aerosols across a wide range of relative humidities. Journal of Physical Chemistry A, 110(24), 7614–7620. 10.1021/jp060639a [PubMed: 16774205]

Shang D, Peng J, Guo S, Wu Z, & Hu M (2021). Secondary aerosol formation in winter haze over the Beijing-Tianjin-Hebei region, China. Frontiers of Environmental Science and Engineering, 15(2), 34. 10.1007/s11783-020-1326-x

Simon H, Kimura Y, McGaughey G, Allen D, Brown S, Osthoff H, et al. (2009). Modeling the impact of $ClNO_2$ on ozone formation in the Houston area. Journal of Geophysical Research, 114(D7), D00F03. 10.1029/2008JD010732

Skamarock WC, Klemp JB, Dudhia J, Grill DO, Barker DM, Duda MG, et al. (2008). A description of the advanced research WRF version 3 NCAR Tech Note NCAR/TN 475 STR (p. 125). 10.5065/D68S4MVH

Su X, Tie XX, Li GH, Cao JJ, Huang RJ, Feng T, et al. (2017). Effect of hydrolysis of N_2O_5 on nitrate and ammonium formation in Beijing China: WRF-chem model simulation. Science of the Total Environment, 579, 221–229. 10.1016/j.scitotenv.2016.11.125 [PubMed: 27890411]

Tanaka PL, Oldfield S, Neece JD, Mullins CB, & Allen DT (2000). Anthropogenic sources of chlorine and ozone formation in urban atmospheres. Environmental Science and Technology, 34(21), 4470–4473. 10.1021/es991380v

Tanaka PL, Riemer DD, Chang S, Yarwood G, Mcdonald-Buller EC, Apel EC, et al. (2003). Direct evidence for chlorine-enhanced urban ozone formation in Houston, Texas. Atmospheric Environment, 37(9–10), 1393–1400. 10.1016/S1352-2310(02)01007-5

Tham YJ, Wang Z, Li QY, Yun H, Wang WH, Wang XF, et al. (2016). Significant concentrations of nitryl chloride sustained in the morning: Investigations of the causes and impacts on ozone production in a polluted region of northern China. Atmospheric Chemistry and Physics, 16(23), 14959–14977. 10.5194/acp-16-14959-2016

Wang L, Arey J, & Atkinson R (2005). Reactions of chlorine atoms with a series of aromatic hydrocarbons. Reactions of Chlorine Atoms with a Series of Aromatic Hydrocarbons, 39(14), 5302–5310. 10.1021/es0479437

Wang X, Jacob DJ, Eastham SD, Sulprizio MP, Zhu L, Chen Q, et al. (2019). The role of chlorine in global tropospheric chemistry. Atmospheric Chemistry and Physics, 19(6), 3981–4003. 10.5194/acp-19-3981-2019

Wang X, Jacob DJ, Fu X, Wang T, Breton ML, Hallquist M, et al. (2020). Effects of anthropogenic chlorine on $PM_{2.5}$ and ozone air quality in China. Environmental Science and Technology, 54(16), 9908–9916. 10.1021/acs.est.0c02296 [PubMed: 32600027]

Xia M, Peng X, Wang WH, Yu C, Sun P, Li YY, et al. (2020). Significant production of $ClNO_2$ and possible source of Cl_2 from N_2O_5 uptake at a suburban site in eastern China. Atmospheric Chemistry and Physics, 20(10), 6147–6158. 10.5194/acp-20-6147-2020

Yarwood G, Jung J, Whitten GZ, Heo G, Mellberg J, & Estes M (2010). Updates to the carbon bond mechanism for version 6 (CB6).

Yi X, Sarwar G, Bian J, Li QY, Jiang S, Liu HQ, et al. (2023). Significant impact of reactive chlorine on complex air pollution over the Yangtze River Delta region [Dataset]. Zenodo. 10.5281/zenodo.7997238

Yi X, Yin SJ, Huang L, Li HL, Wang YJ, Wang Q, et al. (2021). Anthropogenic emissions of atomic chlorine precursors in the Yangtze River Delta region, China. Science of the Total Environment, 771, 144644. 10.1016/j.scitotenv.2020.144644 [PubMed: 33736175]

Yin SJ, Yi X, Li L, Huang L, Chel Gee Ooi M, Wang YJ, et al. (2022). An updated anthropogenic emission inventory of reactive chlorine precursors in China. ACS Earth and Space Chemistry, 6(7), 1846–1857. 10.1021/acsearthspacechem.2c00096

Zelenov VV, Aparina EV, & Ivanov AV (2014). Time-dependent uptake of NO_3 by sea salt. Journal of Atmospheric Chemistry, 1(1), 1–10. 10.1007/s10874-014-9279-8

Zhang L, Li QY, Wang T, Ahmadov R, Zhang Q, Li M, & Lv M (2017). Combined impacts of nitrous acid and nitryl chloride on lower-tropospheric ozone: New module development in WRF-chem and application to China. Atmospheric Chemistry and Physics, 17(16), 9733–9750. 10.5194/acp-17-9733-2017

Zhang SP, Sarwar G, Xing J, Chu BW, Xue CY, Sarav A, et al. . (2021). Improving the representation of HONO chemistry in CMAQ and examining its impact on haze over China. Atmospheric Chemistry and Physics, 21(20), 15809–15826. 10.5194/acp-21-15809-2021 [PubMed: 34804135]

Zhang YZ, Liu JF, Tao W, Xiang SL, Liu HZ, Yi K, et al. (2020). Impacts of chlorine emissions on secondary pollutants in China. Atmospheric Environment, 246, 118177. 10.1016/j.atmosenv.2020.118177

Zhou M, Zheng G, Wang H, Qiao L, Zhu S, Huang D, et al. (2022). Long-term trends and drivers of aerosol pH in eastern China. Atmospheric Chemistry and Physics, 22(20), 13833–13844. 10.5194/acp-22-13833-2022

Key Points:

- The impact of new chlorine emissions from disinfectant usage in the Weather Research and Forecasting-Community Multiscale Air Quality (WRF-CMAQ) model was evaluated against observations in the Yangtze River Delta
- The Cl chemistry of WRF-CMAQ was updated by adding 21 new reactions, including 13 gas-phase and eight heterogeneous reactions
- Chlorine chemistry has different impacts on O3 and PM2.5 in different seasons, with higher impacts found in autumn and winter

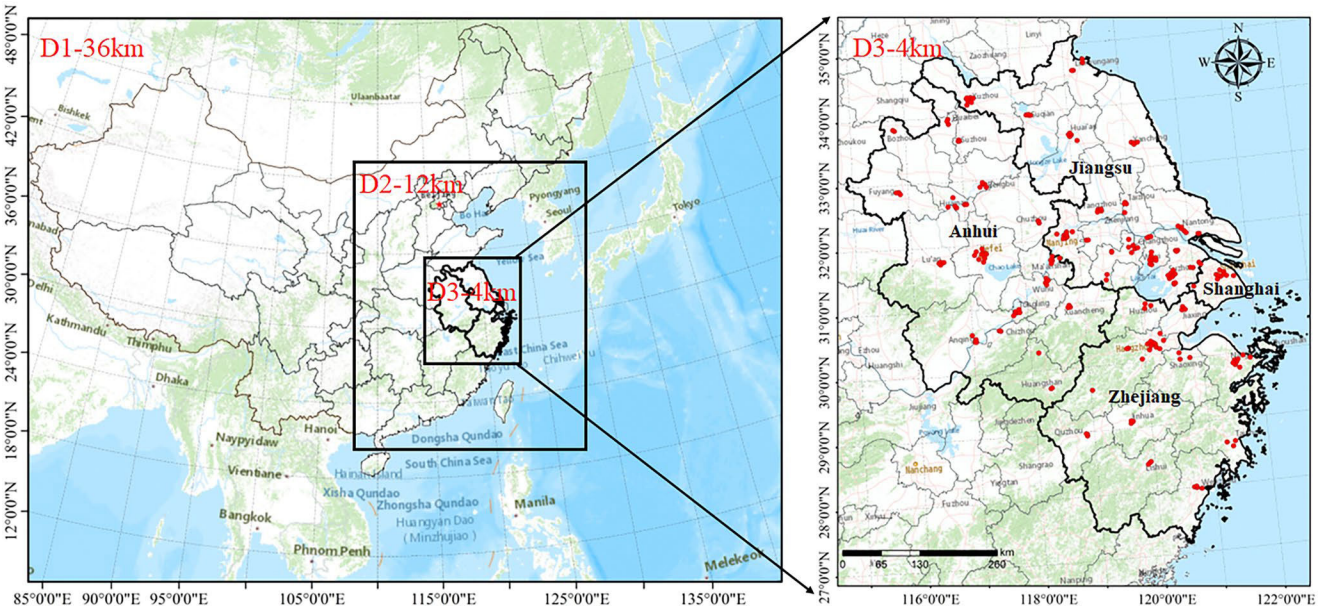

Figure 1.

The simulation domain for the WRF-CMAQ model. The red dots represent the surface air quality monitoring stations.

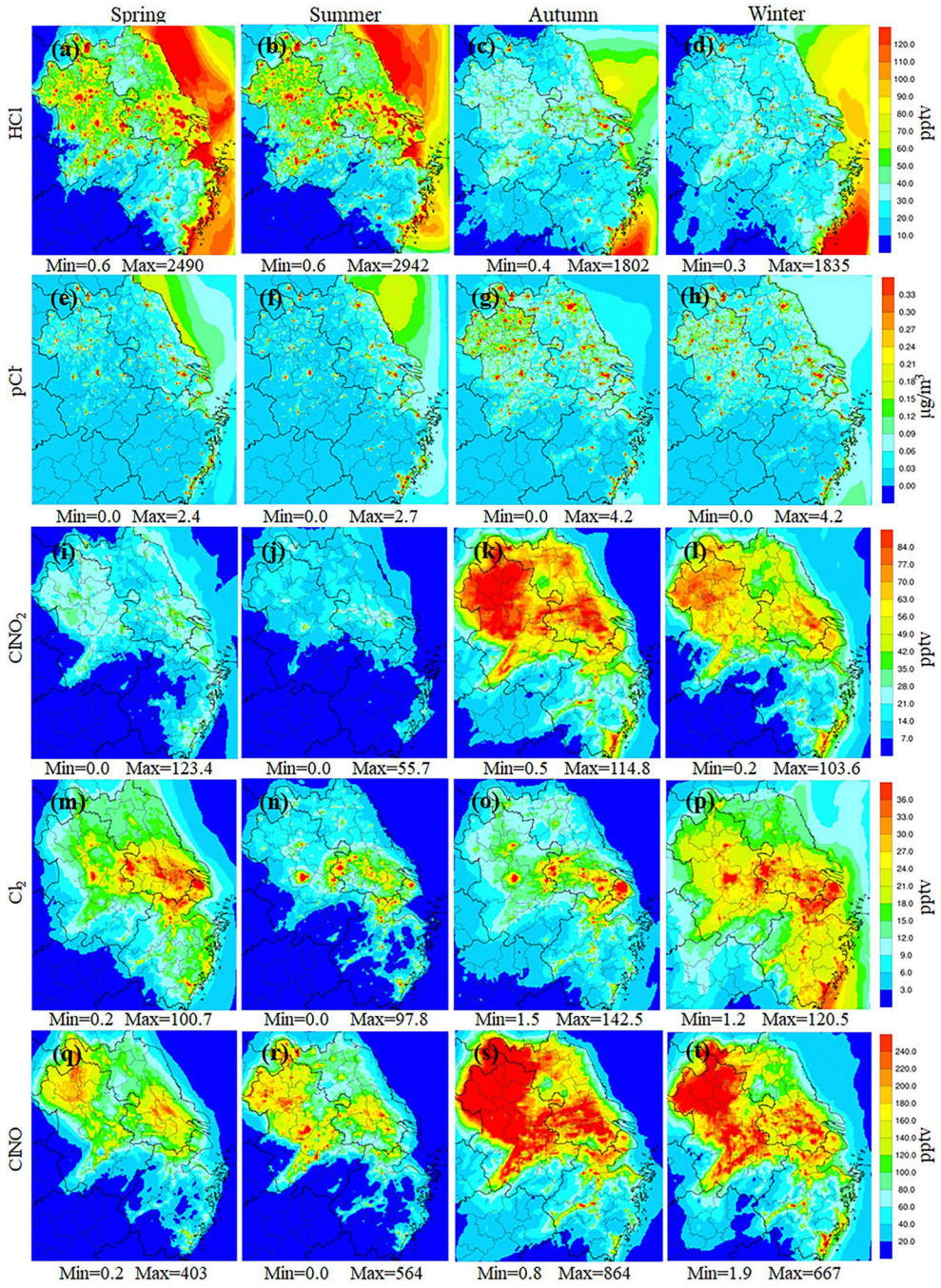

Figure 2.

Monthly average HCl, pCl^-, $ClNO_2$, Cl_2, and ClNO concentration during different seasons in 2018 in the CL experiment.

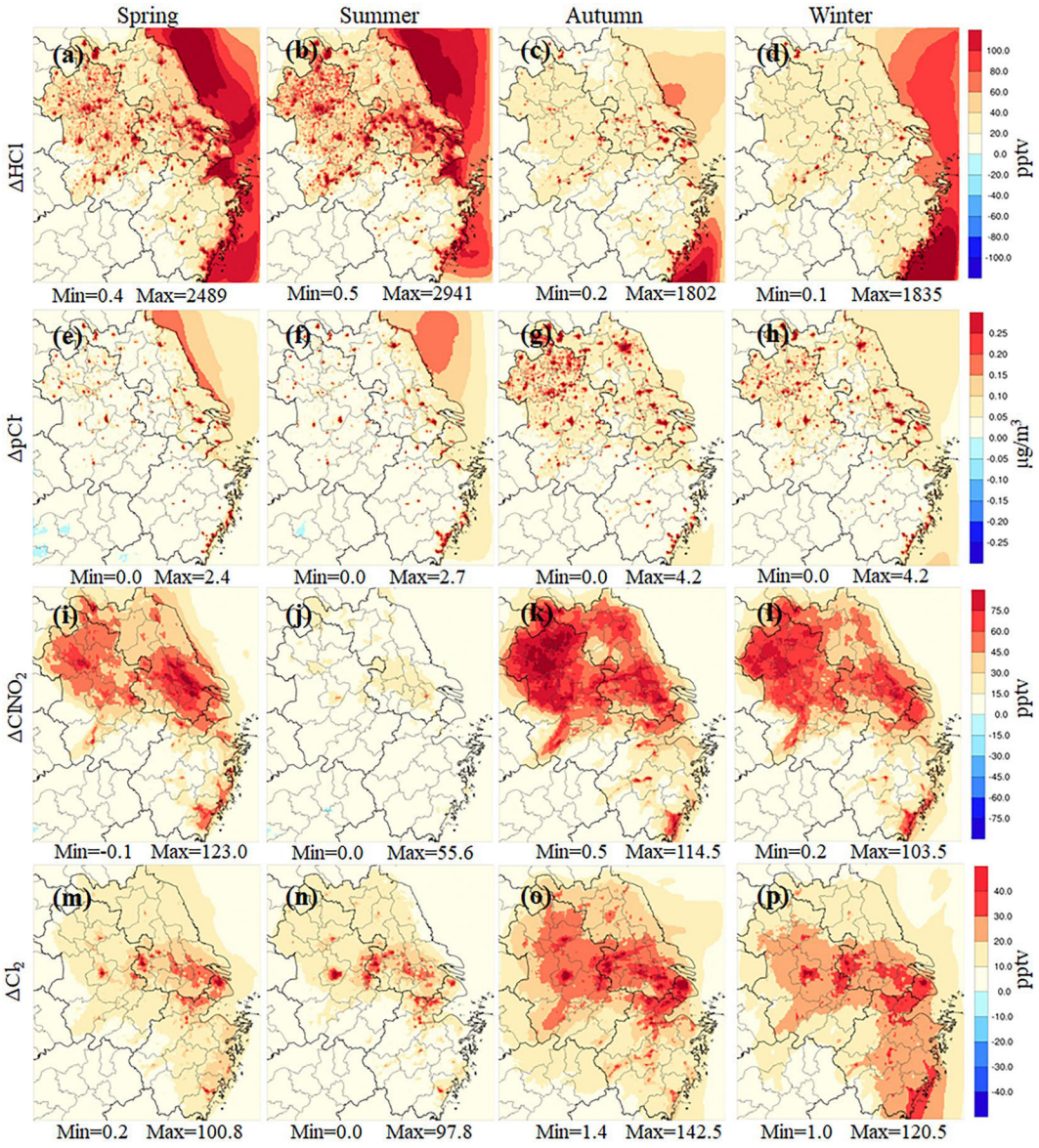

Figure 3.

Differences in monthly average HCl, pCl^-, $ClNO_2$, and Cl_2 between the CL experiment and the Base experiment (CL-Base) in different seasons in 2018.

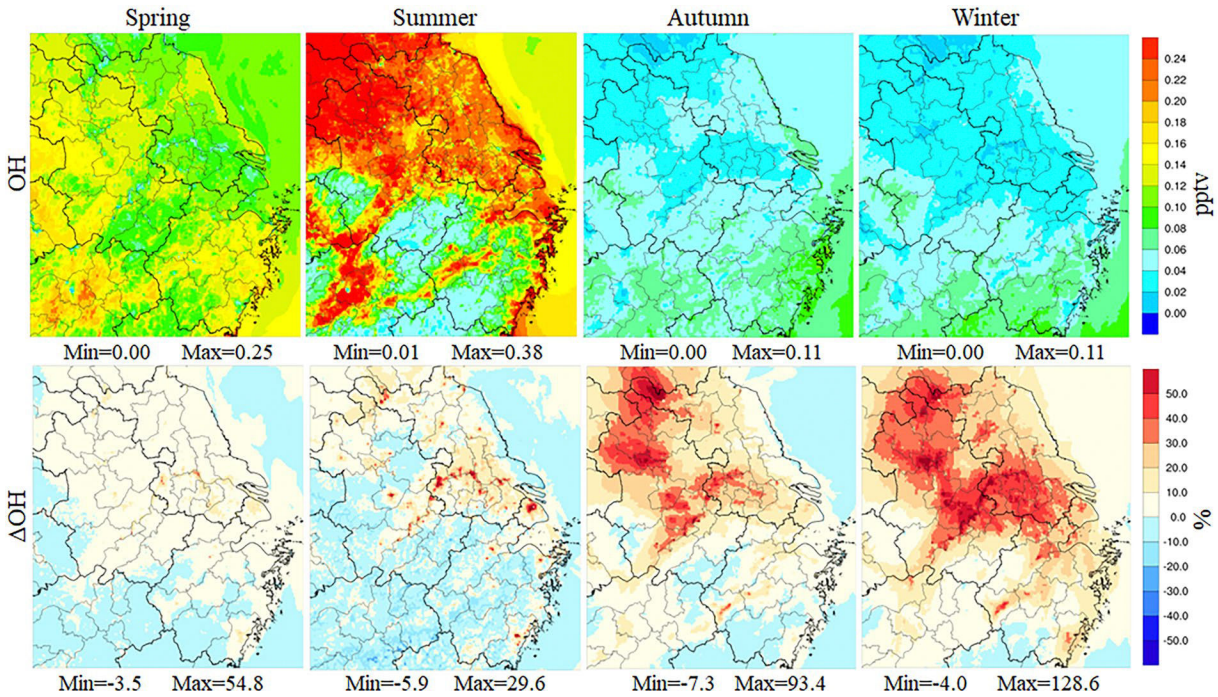

Figure 4.

Simulated monthly average of OH in the Base experiment, relative changes ((CL-Base)/Base) due to the chlorine chemistry in different seasons in 2018.

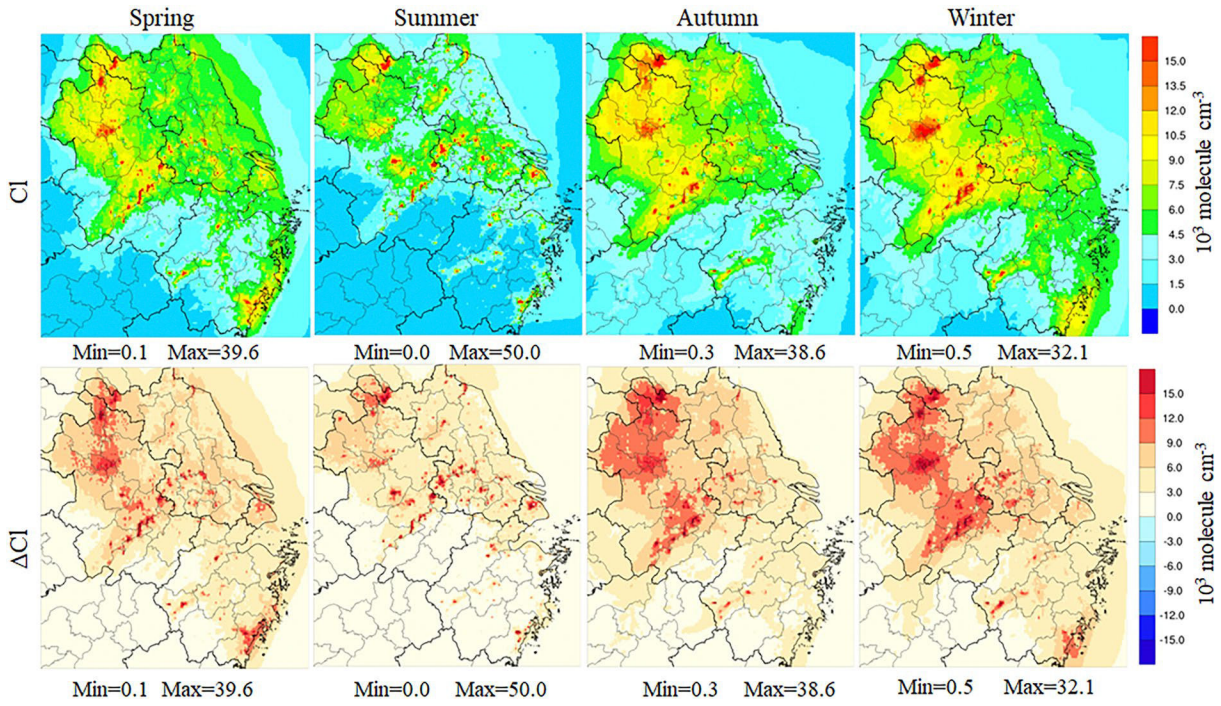

Figure 5.

Simulated monthly average of Cl in the CL experiment, changes (CL-Base) due to the implementation of chlorine chemistry in different seasons in 2018.

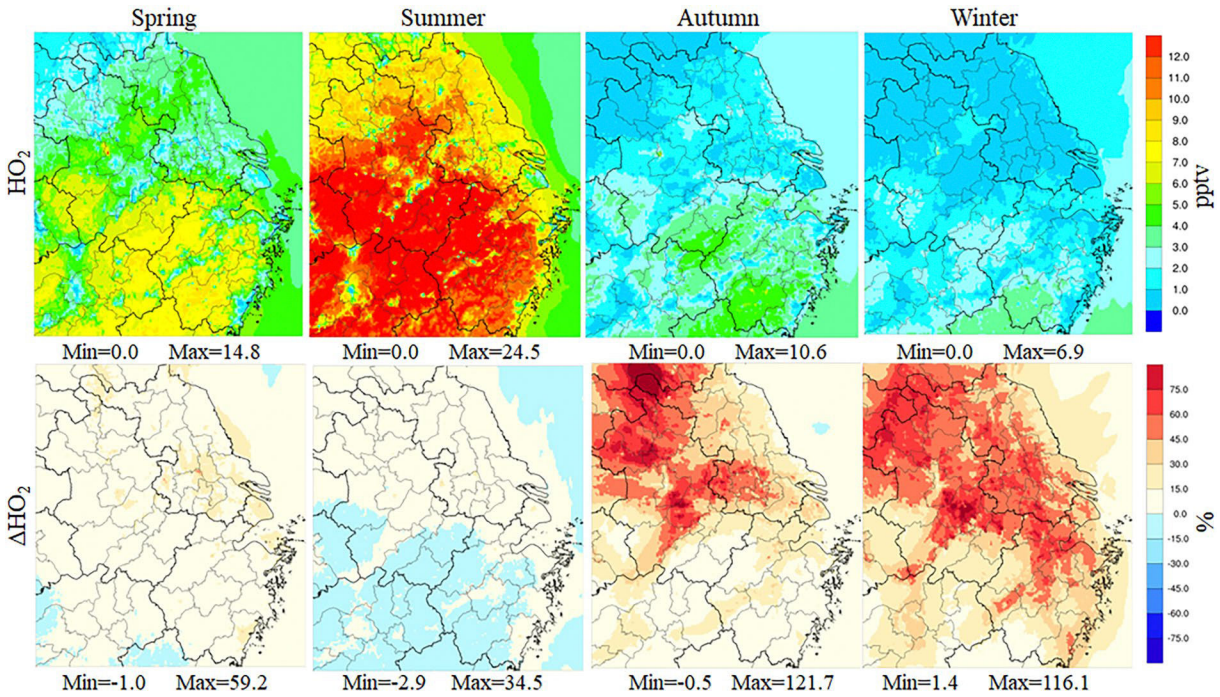

Figure 6.

Simulated monthly average of HO_2 in the Base experiment, relative changes ((CL-Base)/Base) due to the chlorine chemistry in different seasons in 2018.

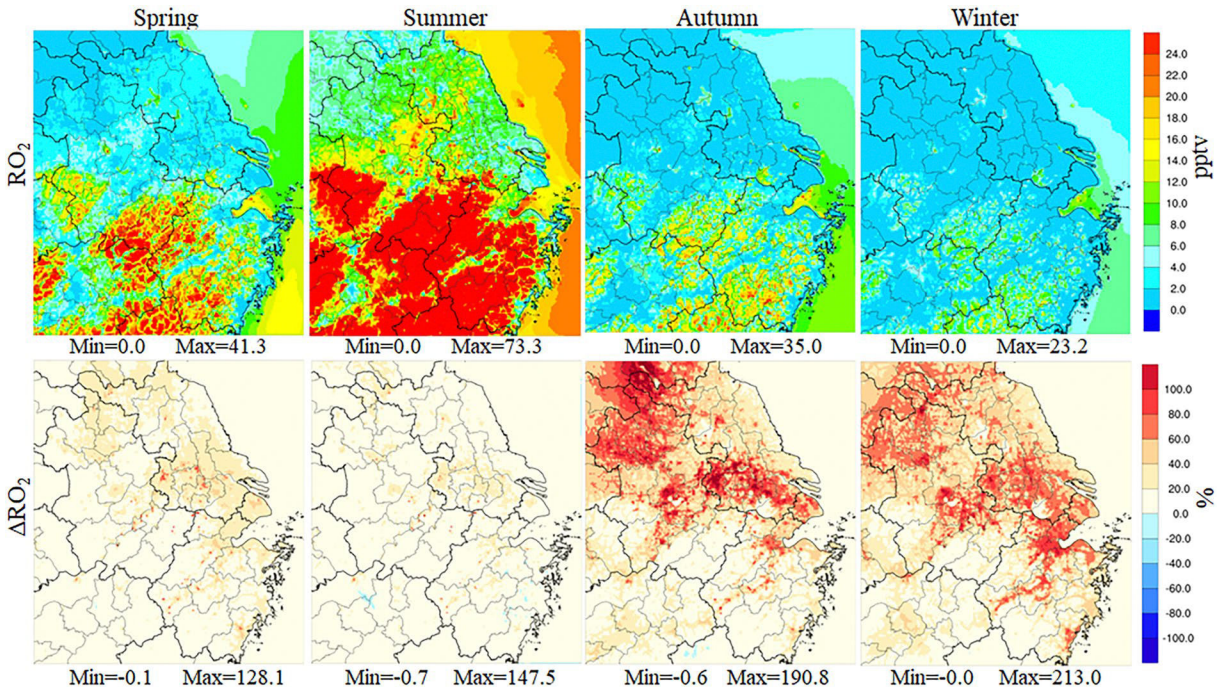

Figure 7.

Simulated monthly average of RO_2 in the Base experiment, relative changes ((CL-Base)/Base) due to the chlorine chemistry in different seasons in 2018.

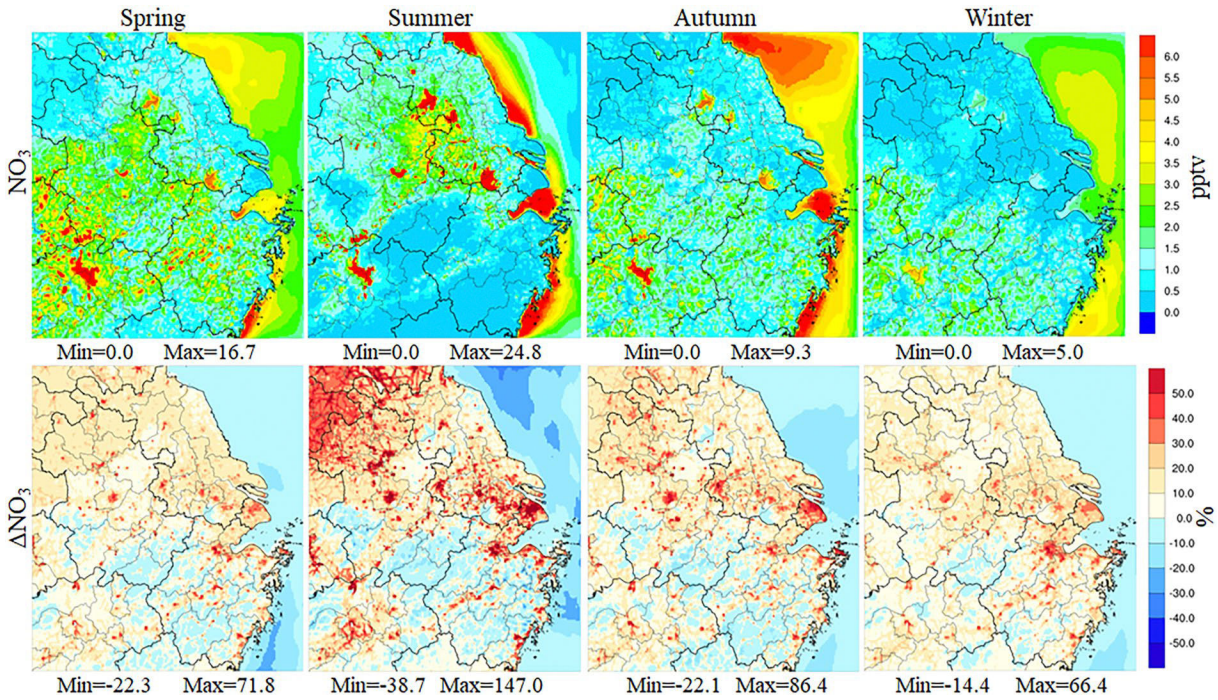

Figure 8.

Simulated monthly average of NO_3 in the Base case, relative changes ((CL-Base)/Base) due to the chlorine chemistry in different seasons in 2018.

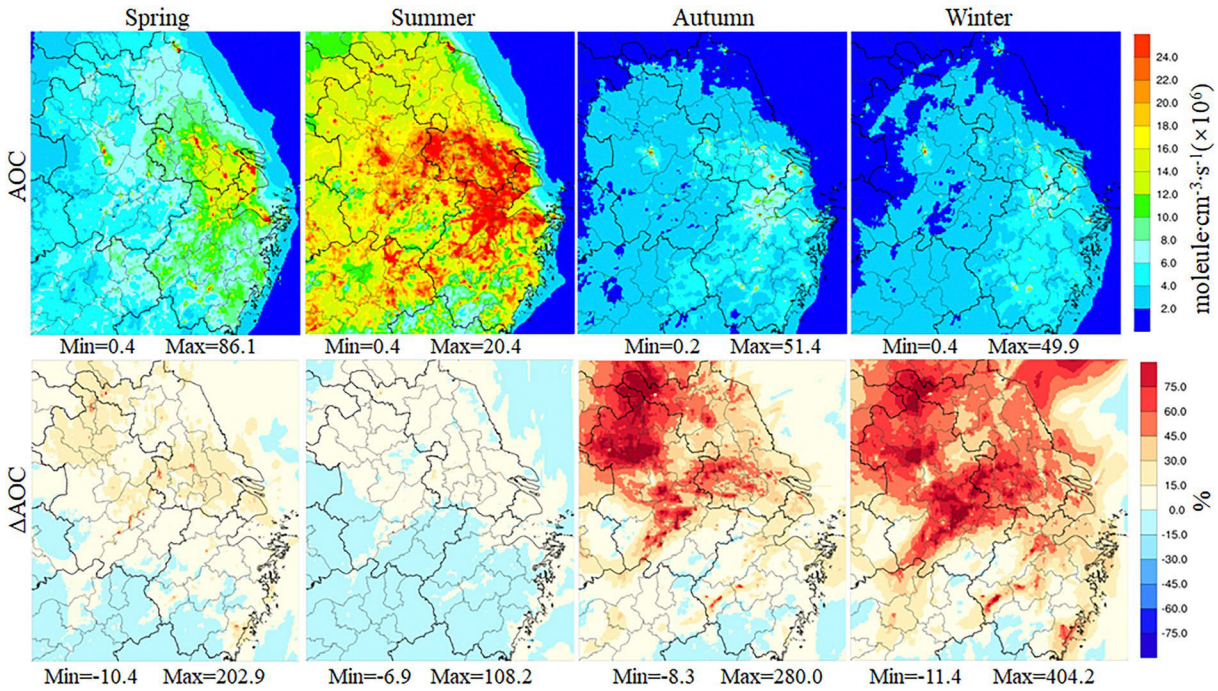

Figure 9.

Simulated monthly average of atmospheric oxidative capacity in the Base experiment, relative changes ((CL-Base)/Base) due to the chlorine chemistry in different seasons in 2018.

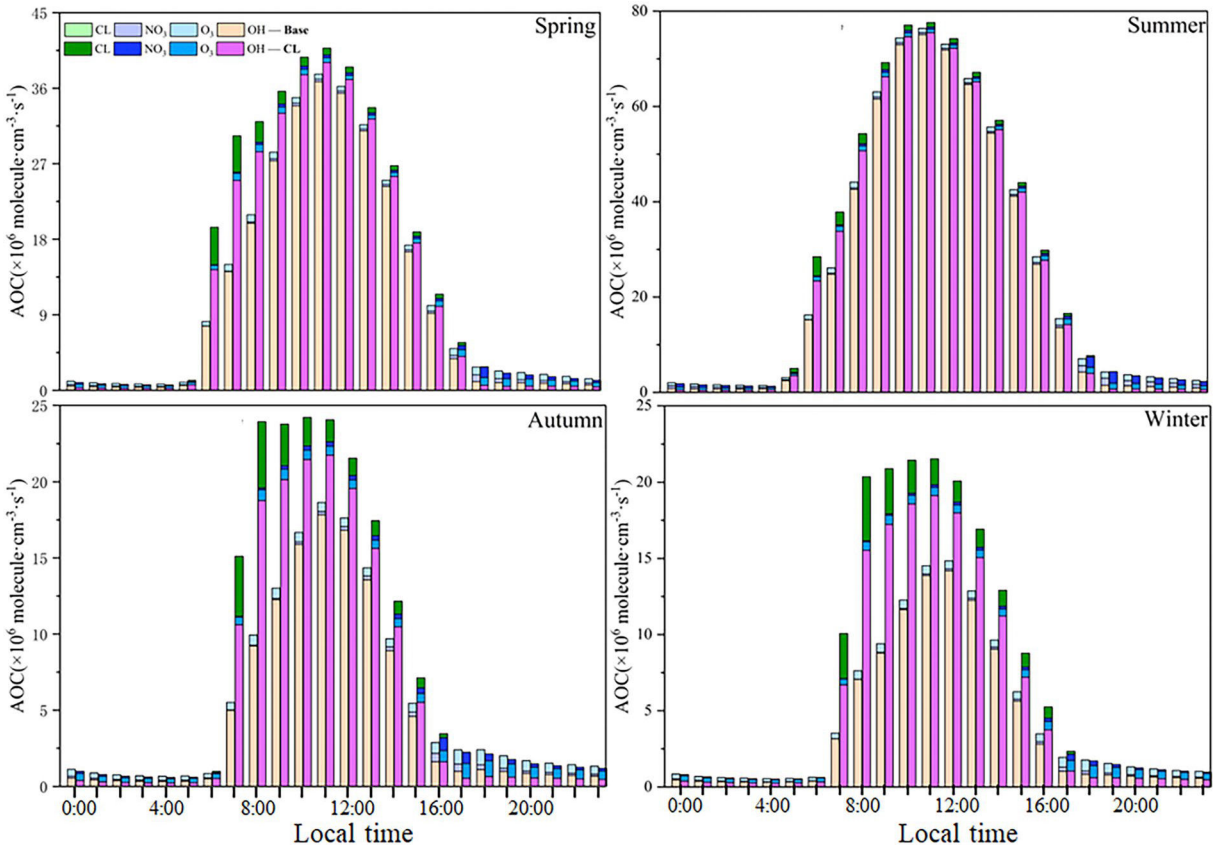

Figure 10.

Simulated averaged hourly atmospheric oxidative capacity in Yangtze River Delta in different seasons.

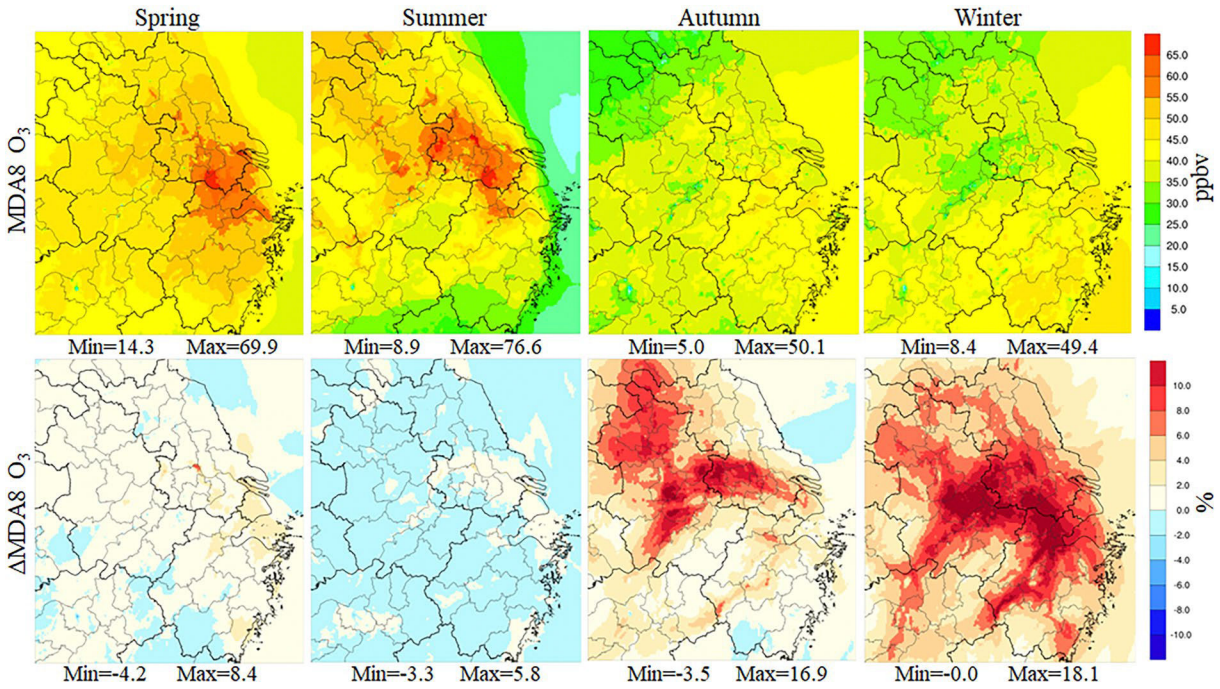

Figure 11.

Simulated monthly average of MDA8 O_3 in the Base case, changes ((CL-Base)/Base) due to the chlorine chemistry during different seasons in 2018.

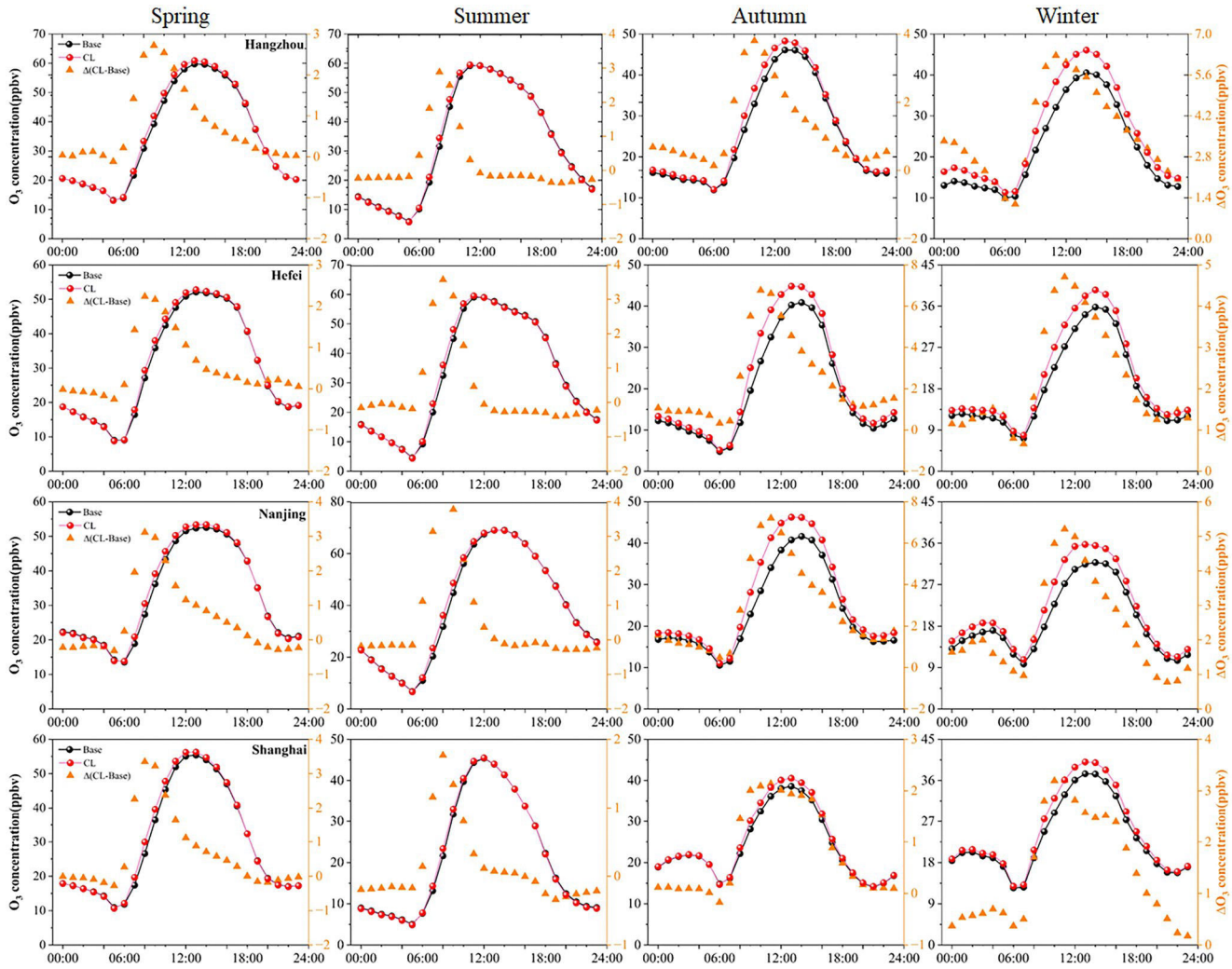

Figure 12.
Effects of chlorine emission on time distribution of O_3 in major cities.

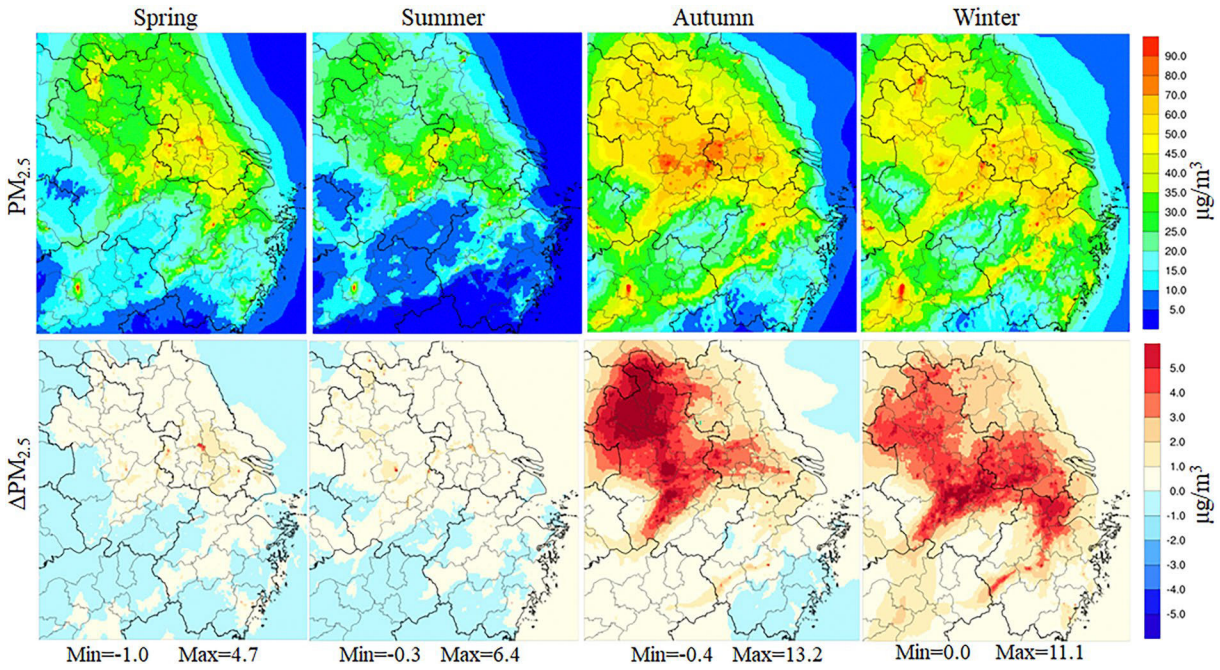

Figure 13.

Simulated monthly average of $PM_{2.5}$ in the Base experiment, changes (CL-Base) between the CL and Base experiment in different seasons in 2018.

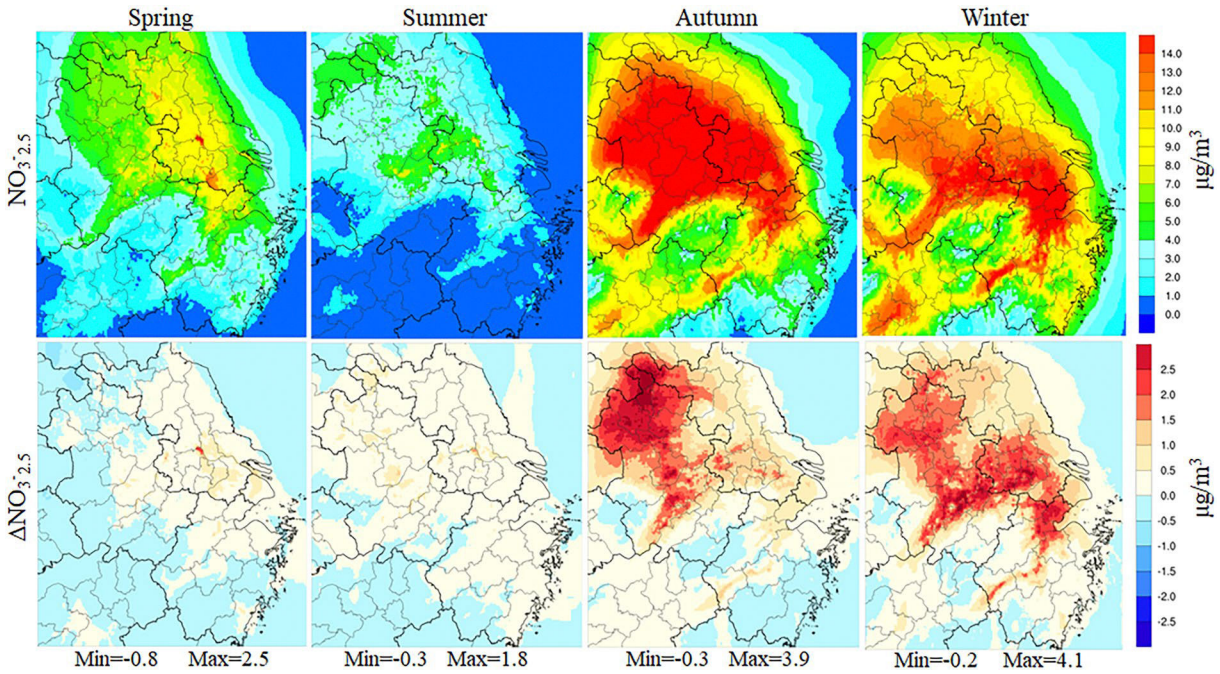

Figure 14.

Simulated monthly average of $NO_3^-_{2.5}$ in the Base case, changes (CL-Base) between the CL and Base experiment in different seasons in 2018.

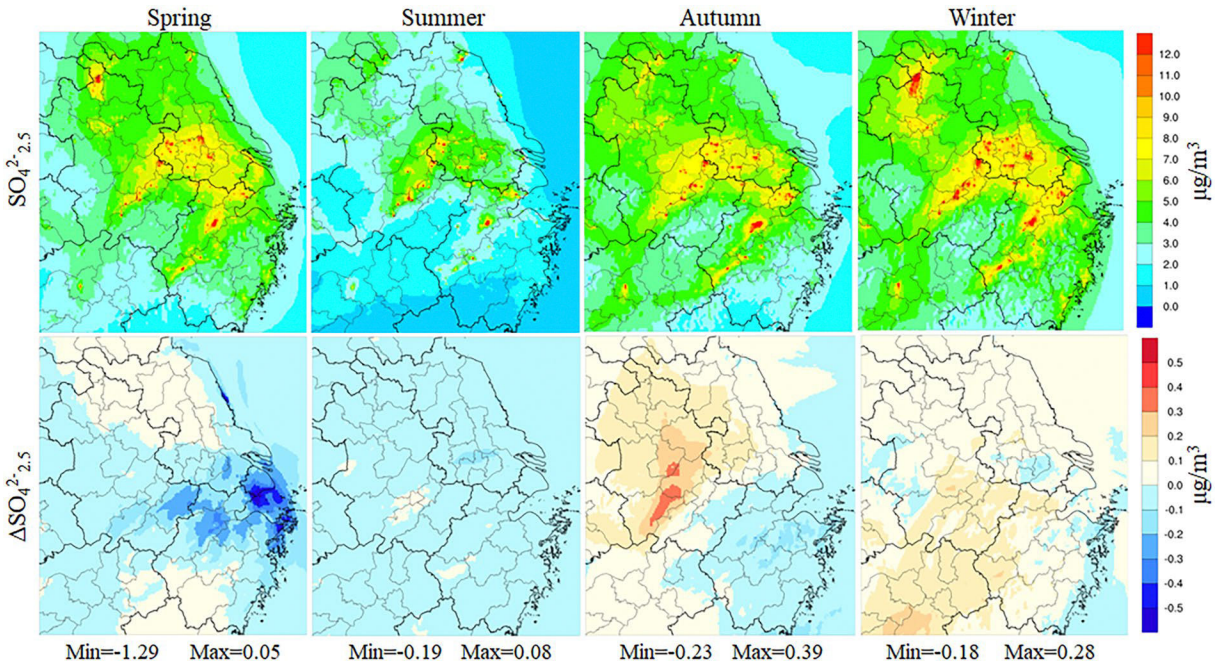

Figure 15.

Simulated monthly average of $SO_4^{2-}{}_{2.5}$ in the Base experiment, changes (CL-Base) between the CL and Base experiment in different seasons in 2018.

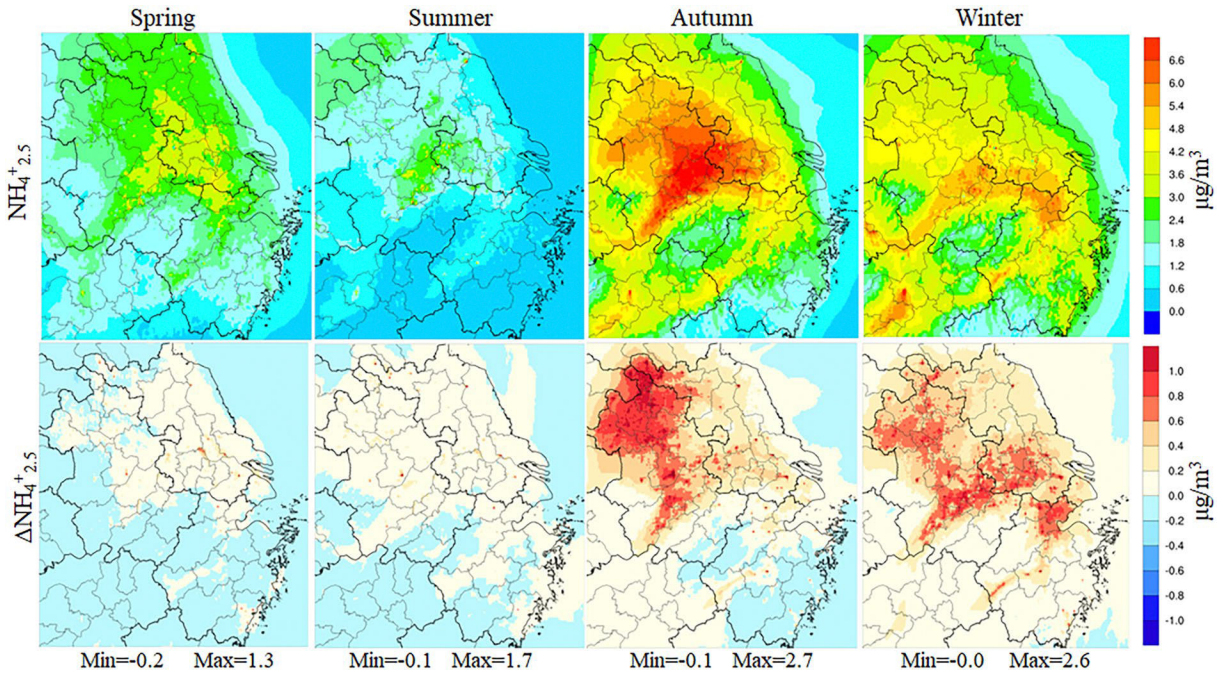

Figure 16.

Simulated monthly average of $NH_4^+{}_{2.5}$ in the Base case, changes (CL-Base) between the CL and Base experiment in different seasons in 2018.

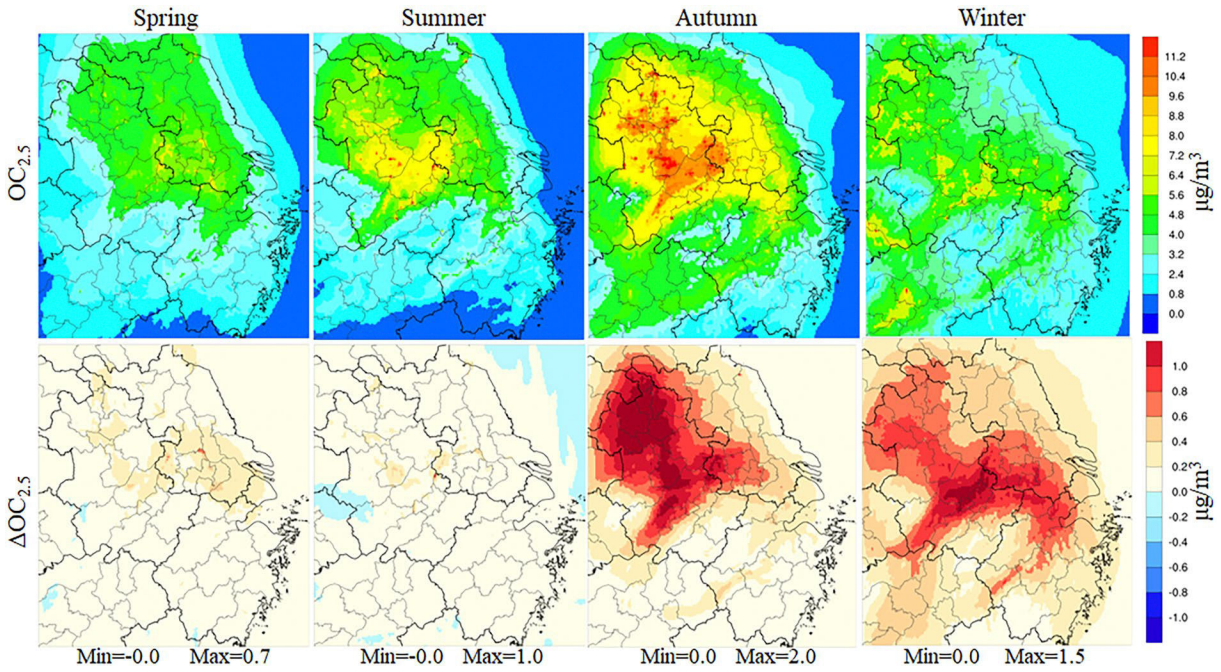

Figure 17.

Simulated monthly average of $OC_{2.5}$ in the Base case, changes (CL-Base) between the CL and Base experiment in different seasons in 2018.

Table 1

Model Performance Evaluation for $PM_{2.5}$, and O_3 in February, April, July, and November 2018

			Sim		MB		rmse		IOA		r	
Items	**Month**	**Obs**	**Base**	**CL**	**Base**	**CL**	**Base**	**CL**	**Base**	**CL**	**Base**	**CL**
O_3 (μg/m^3)	Feb	56.9	48.4	53.3	−8.6	−3.7	31.3	33.3	0.67	0.65	0.50	0.45
	Apr	84.9	70.7	71.9	−14.2	−13.0	41.4	42.3	0.79	0.78	0.70	0.68
	Jul	69.7	65.2	65.6	−4.5	−4.1	37.0	37.8	0.82	0.81	0.70	0.69
	Nov	44.8	52.3	55.3	7.6	10.5	33.7	36.5	0.67	0.64	0.50	0.46
$PM_{2.5}$ (μg/m^3)	Feb	58.9	54.2	58.2	−4.7	−0.7	37.2	38.6	0.74	0.74	0.61	0.62
	Apr	47.1	40.0	40.8	−7.1	−6.3	28.5	29.1	0.69	0.68	0.56	0.56
	Jul	23.7	26.2	26.8	2.5	3.2	22.5	23.4	0.52	0.51	0.34	0.34
	Nov	51.5	51.8	54.9	0.4	3.5	41.4	43.4	0.73	0.72	0.65	0.64

Note. Obs: average concentration of observation; Sim: average concentration of simulation; MB: mean bias; RMSE: root mean square error; IOA: index of agreement; r: correlation coefficient.

Table 2

Observed and Model-Predicted Chlorine-Containing Substances in the CL Experiment

Species	Location	Period	Concentration (Avg)	Ref.
HCl ($\mu g/m^3$)	Changzhou, China	Feb, 2018	0.13	Super station
			0.02(Sim)	This study
		Apr. 2018	0.18	Super station
			0.08(Sim)	This study
		Jul, 2019	0.24	Super station
		Jul. 2018	0.09(Sim)	This study
		Nov. 2018	0.24	Super station
			0.07(Sim)	This study
pCl^- ($\mu g/m^3$)	Changzhou, China	Feb. 2018	2.95	Super station
			0.10(Sim)	This study
		April 2018	1.36	Super station
			0.07(Sim)	This study
		July 2019	0.93	Super station
		July 2018	0.09(Sim)	This study
		Nov 2018	2.09	Super station
			0.1(Sim)	This study
$ClNO_2$ (ppt)	Nanjing, China	Apr. 2018	3,700 (1 min max)	Xia et al. (2020)
		Apr. 2018	368 (1 hr max)	This study
Cl_2 (ppt)	Nanjing, China	Apr. 2018	100 (1 min max)	Xia et al. (2020)
		Apr. 2018	220 (1 hr max)	This study
HOCl(ppt)	Nanjing, China	Apr. 2018	~200	Xia et al. (2020)
		Apr. 2018	125	This study

Table 3

Comparisons With Previous Studies

Region	Time	Model	New chlorine mechanism	Precursor	1 h O_3 (ppbv)	8 h O_3 (ppbv)	OH (%)	AOC(%)	$NO_3^-{}_{2.5}$ (μg/m^3)	$PM_{2.5}$ (μg/m^3)	Reference
Texas	1993.09	CAMx	No	Cl_2	~16	—	—	—	—	—	Chang et al. (2002)
Texas	2000.08–09	CAMx	No	Cl_2	~16	—	—	—	—	—	Tanaka et al. (2003)
California	1993.09	CACM	Yes	Seasalt	~12	—	—	—	—	—	Knipping & Dabdub (2003)
Texas	2000.08–09	CAMx	Yes	Cl_2	~72	~21	—	—	—	—	Chang & Allen (2006)
Eastern USA	2001.07	CMAQ	Yes	Cl_2,HOCl	~12	~8	—	—	—	—	Sarwar and Bhave (2007)
Texas	2006.07	CAMx	Yes	$ClNO_2$	1.5	—	—	—	—	—	Simon et al. (2009)
Continental USA	2006.09	CMAQ	Yes	Cl_2,HCl,pCl^-	—	~13	—	—	—	—	Sarwar et al. (2012)
Northern	2006.01	CMAQ	Yes	$ClNO_2$	—	~7	3.5	—	—	—	Sarwar et al. (2014)
Hemisphere	2006.06					~1.6	0.3	—	—	—	
HK–PRD	2013.12	WRF-Chem	Yes	HCl,pCl^-	~7.23	—	—	—	~13.45	—	Q. Fi et al. (2016)
Wangdu	2014.07	MCM	Yes	$ClNO_2$	~11	—	—	—	—	—	Tham et al. (2016)
NCP/YRD	2014.07	WRF-Chem	Yes	HCl,pCl^-	~3.3	—	—	—	—	—	Zhang et al. (2017)
China	2011.11	WRF-CMAQ	No	Cl_2,HCl,pCl^-	~7.7	~2	—	—	—	—	Fiu et al. (2018)
Northern China	2014.07	CMAQ	Yes	Cl_2,HCl,pCl^-	20%	—	28	—	—	—	Qiu et al. (2019a)
China	2014 (year)	GEOS-Chem	Yes	HCl,pCl^-	~1.9	—	—	—	—	~3.2	Wang et al. (2020)
eastern China	2015.01	CMAQ	Yes	Cl_2,HCl	0 ~ 34.3	−0.2 ~ 4.9	—	—	—	—	Hong et al. (2020)
	2015.04				0 ~ 13.2	0 ~ 1.5	—	—	—	—	
	2015.07				0 ~ 11.5	−0.1 ~ 1	—	—	—	—	
	2015.10				0 ~ 16.4	−0.1 ~ 2.8	—	—	—	—	

Region	Time	Model	New chlorine mechanism	Precursor	1 h O_3 (ppbv)	8 h O_3 (ppbv)	OH (%)	AOC(%)	NO_3^- 2.5 (μg/m^3)	$PM_{2.5}$ (μg/m^3)	Reference
YRD	2018.05~06	CMAQ	Yes	Cl_2,HCl,pCl^-	—	—	−5.3 ~ 36.6 (day)8.9 ~ 104.1 (night)	—	—	—	J. Y. Fi et al. (2021)
China	2014.07	WRF-Chem	Yes	HCl,pCl^-	—	−2~ −8	—	—	—	—	Zhang et al. (2021)
	2014.11				—	−3.5~−0.5	—	—	−2.5~	~7.5	
YRD	2018.02	CMAQ	Yes	Cl_2,HOCl,HCl,pCl^-	−0.2 ~ 7.4	−0.0 ~ 6.7	−4.0 ~ 128.6	−11.4 ~ 404.2	−0.2 ~ 4.1	−0.0~11.1	This research
	2018.04				−0.8 ~ 10.3	−0.7 ~ 4.6	−3.5 ~ 54.8	−10.4 ~ 202.9	−0.8 ~ 2.5	−1.0~4.7	
	2018.07				−0.7 ~ 12.0	−0.7 ~ 4.1	−5.9 ~ 29.6	−6.9 ~ 108.2	−0.3 ~ 1.8	−0.3~6.4	
	2018.11				−0.5 ~ 8.4	−0.3 ~ 7.0	−7.3 ~ 93.4	−8.3 ~ 280.0	−0.3 ~ 3.9	−0.4~13.2	